



Original article

Development of quinone analogues as dynamin GTPase inhibitors



Kylie A. MacGregor^{a,2}, Mohammed K. Abdel-Hamid^{a,c,2}, Luke R. Odell^{a,1}, Ngoc Chau^b, Ainslie Whiting^b, Phillip J. Robinson^b, Adam McCluskey^{a,*}

^a Centre for Chemical Biology, Chemistry, School of Environmental and Life Sciences, The University of Newcastle, Callaghan, NSW 2308, Australia

^b Children's Medical Research Institute, University of Sydney, Westmead, NSW 2145, Australia

^c Department of Medicinal Chemistry, Faculty of Pharmacy, Assiut University, Assiut 71526, Egypt

ARTICLE INFO

Article history:

Received 6 March 2014

Received in revised form

27 June 2014

Accepted 28 June 2014

Available online 5 July 2014

Keywords:

Dynamin

Endocytosis

Quinones

Dynamin inhibitors

Modelling

ABSTRACT

Virtual screening of the ChemDiversity and ChemBridge compound databases against dynamin I (dynI) GTPase activity identified 2,5-bis-(benzylamino)-1,4-benzoquinone **1** as a $273 \pm 106 \mu\text{M}$ inhibitor. In silico lead optimization and focused library-led synthesis resulted in the development of four discrete benzoquinone/naphthoquinone based compound libraries comprising 54 compounds in total. Sixteen analogues were more potent than lead **1**, with 2,5-bis-(4-hydroxyanilino)-1,4-benzoquinone (**45**) and 2,5-bis(4-carboxyanilino)-1,4-benzoquinone (**49**) the most active with IC_{50} values of 11.1 ± 3.6 and $10.6 \pm 1.6 \mu\text{M}$ respectively. Molecular modelling suggested a number of hydrogen bonding and hydrophobic interactions were involved in stabilization of **49** within the dynI GTP binding site. Six of the most active inhibitors were evaluated for potential inhibition of clathrin-mediated endocytosis (CME). Quinone **45** was the most effective CME inhibitor with an $\text{IC}_{50(\text{CME})}$ of $36 \pm 16 \mu\text{M}$.

Crown Copyright © 2014 Published by Elsevier Masson SAS. All rights reserved.

1. Introduction

Dynamin GTPase belongs to the dynamin super-family of large GTPases which play crucial roles in the catalysis of membrane fission during clathrin mediated endocytosis (CME), regulation of cellular actin dynamics and are important for cytokinesis [1]. There are three classical dynamins (dynI, dynII and dynIII) which each have low affinity for guanine nucleotides ($10\text{--}100 \mu\text{M}$), high basal GTP turnover ($0.4\text{--}1 \text{min}^{-1}$) and the propensity for oligomerization into helical arrays around a template [2]. Each dynamin comprises five structural domains including an amino-terminal G domain that binds and hydrolyses GTP, a middle domain involved in self-assembly and oligomerization, a pleckstrin homology (PH) domain responsible for interactions with the plasma membrane and inducing the hemifission state, a GTPase effector domain (GED) which is also involved in self-assembly, and a proline- and arginine-rich (PRD) domain that interacts with SH3 domains in accessory proteins [3–5]. With the exception of the PRD, tertiary structures of all dynamin's individual domains have been reported [6–9]. In

particular, two crystal structures for the near full length mammalian dynI (lacking the PRD domain) have been solved, providing valuable information regarding the complex dynamics involved in dynamins' GTPase cycle and its role as a fission protein in cells [10,11].

CME is a highly regulated cellular process in which growth factors and membrane-bound receptors are concentrated in invaginating clathrin-coated pits (CCPs). These CCPs pinch off to form vesicles which carry the cargo into the cell [10]. In the final stages of CME, dynamin GTPase can assemble into collars at the necks of the deeply invaginated CCPs to catalyse membrane fission apparently by neck constriction [3,11,12]. Synaptic vesicle endocytosis (SVE) in neural cells is based on a similar mechanism to CME and plays a role in the internalization of membrane to allow synaptic vesicle recycling thus sustaining synaptic transmission [11]. SVE and CME differ mainly in the dynamin genes that are utilized in each case and unique regulation of SVE by protein dephosphorylation. While dynII is found throughout the body and is the major scission protein for CME, dynI is mainly found in neuronal cells where it coexists with dynII and dynIII. In neural cells dynI protein is expressed at about 50-fold higher levels than the two other classical dynamins and is critical for neural cell functions [1].

We have previously reported the identification and development of the MiTMAB [13], Bis-T [14,15], RTIL [16], IminiodynTM [17], PthaladynTM [18], DyngoTM [19,20], RhodadynTM [21] series and two generations of DynoleTM [22–24] compounds as dynamin

* Corresponding author.

E-mail address: Adam.McCluskey@newcastle.edu.au (A. McCluskey).

¹ Current address: Organic Pharmaceutical Chemistry, Department of Medicinal Chemistry, Uppsala Biomedical Centre, Uppsala University, Box 574, SE-751 23 Uppsala, Sweden.

² These authors contributed equally to this work.

inhibitors [25]. We have also described the virtual screening of the ChemBridge and the ChemDiversity chemical databases against a dynl GTPase domain homology model (hDynl) using ICM flexible ligand-grid receptor algorithm to target the GTP binding site which led to the identification of the Pthalodyn™ compound series [17]. Herein we report on the development of a second series of compounds from our initial virtual screening hits were we identified 2,5-bis-(benzylamino)cyclohexa-2,5-diene-1,4-dione (**1**) as a $273 \pm 106 \mu\text{M}$ potent dynl inhibitor (Fig. 1).

Quinones have been previously explored in a wide range of different drug development pathways with multiple analogues reported to be active in a myriad of different biological screens [26,27]. In our virtual screening approaches, quinones were retained due to their ability to link potential binding elements that would not otherwise be accessed [28,29]. A number of quinones have progressed to clinical trials, e.g. ubiquinone 10, diaziquone, mitoxantrone hydrochloride and monobenzene [29]; and in a related area (to this study) the natural product bolinaquinone has been shown to display high levels of specificity towards clathrin [30]. Herein we anticipated that our medicinal chemistry efforts with lead **1**, would add to the SAR of dynamin inhibition already established [13–25,31–33].

2. Results and discussion

Structural optimization of **1** commenced with molecular docking and investigation of its predicted orientation within dynl's GTP-binding site. Docking studies were conducted using AutoDock 4.2 and the dynl-GMPPCP co-crystal structure (PDB: 3ZYC) [3,34]. Examination of the GMPPCP binding pose revealed a number of strong hydrogen bonding interactions between the active site residues and GMPPCP (ESI). The hydrogen bonding interactions were similar to that observed with **1** (ESI). These included a strong hydrogen bond (2.4 Å) between one of the quinone carbonyl moieties and the side chain of the catalytically crucial Ser41 [2]. Other hydrogen bond interactions ranged between moderate and weak (2.8–3.2 Å) and involved the backbones and/or side chains of Ser45, Ser46 and Lys206. One of the terminal phenyl rings showed an arene–cation interaction with the side chain of Lys44, similar to that observed between Lys206 and the GMPPCP guanine core within the published co-crystal. However, compound **1** did not show any of the contacts with amino acids at the “dynamain-specific loop” (residues 236–246) which were present with GMPPCP [3]. The lipophilic/hydrophilic contact surface preference in the GTP active site showed a requirement to balance the hydrophilic/hydrophobic characters in subsequent modified quinone (Fig. 2). While the dynamain-specific loop favoured the presence of hydrophobic contacts (Fig. 2A) the P- and G4-loop region favoured hydrophilic interactions (Fig. 2B).

Our initial modelling studies suggested that 1,4-naphthoquinone analogues would retain the required interactions within the active site and consequently fuller engagement with the key active site residues. Thus, treatment of 1,4-naphthoquinone (**2**)

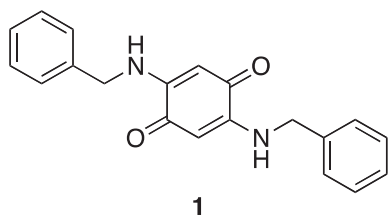


Fig. 1. Chemical structure of virtual screening lead 2,5-bis-(benzylamino)cyclohexa-2,5-diene-1,4-dione (**1**).

and with a range of substituted amines we assembled a discrete library of amine substituted 1,4-naphthoquinones, which were screened for inhibition of dynl GTPase activity (Scheme 1 and Table 1) [35].

Of the 13 analogues synthesized, only **9**, **10** and **12** showed significant improvement in activity compared to the lead **1** ($\text{IC}_{50} = 273 \pm 106 \mu\text{M}$), with IC_{50} values of 30.3, 29.5 and $22.4 \mu\text{M}$ respectively. However, the activity profile for other derivatives was consistent, excepting **6–8**, with the contact preference maps and suggested the symmetry inherent in the parent compound was not absolutely required, but may have bestowed additional features advantageous for dynl inhibition.

The predicted binding poses for the **9**, **10** and **12** showed a high degree of similarity and revealed a number of hydrophobic and hydrogen bonding interactions with the binding site (Fig. 3). One of the quinone carbonyl groups was predicted to accept two hydrogen bonds from P-loop residues, specifically from the backbone and side chain protons of Ser45 and Lys44. The other carbonyl group formed a hydrogen bond with Ser41. The hydroxyl moiety donated a hydrogen bond to either the backbone or the side chain of Arg237 and accepted a Ser46 side chain hydrogen bond. The phenyl substituent made key hydrophobic interactions with the Ala42 and Ile242 side chains, whilst the naphthoquinone core participated in an arene–cation interaction with Lys44 in addition to making hydrophobic contacts with the Ile63, Leu137 and Pro138 side chains. The amine linker donated a moderate strength hydrogen bond to the backbone carbonyl of Gly60.

Given our findings with the naphthoquinone analogues (**3–16**), we next synthesized a focused library of symmetrically substituted *p*-benzoquinone analogues (**1**, **17–33**) (Scheme 2). Treatment of *p*-benzoquinone (**16**) with two equivalents of 2-benzylamine in ethanol at reflux for 18 h [36]. These analogues were screened for their ability to inhibit dynl and these data are presented in Table 2.

Of the *p*-benzoquinone focused library analogues only **18**, **21**, **23** and **33** returned improved activity with dynl IC_{50} values of 29, 170, 112 and $58 \mu\text{M}$, respectively. Only the oxygen bearing benzylamine analogues within this focused library returning IC_{50} values in the 29–170 μM range. The enhanced activity of **18** was attributed to interaction with most key residues at the active site as shown from its “Protein Ligand Interaction Fingerprints” (PLIF, Supplementary data). Although **23** bears a hydroxyl group suggesting a good hydrogen bonding network it showed a lower level of interactions compared to **18** (missing the interaction with Lys44, Gly139 and Asn208) suggesting that the C=O moiety in **18** plays an important role in favourable interactions within the GTP binding site. Methylation of the hydroxyl group giving the 4-methoxy substituted **23** further reduced potency with the loss of the interactions with Gly62 and Val64 in switch I region of the binding site (**21**, $\text{IC}_{50} = 170 \mu\text{M}$). This highlighted the potential importance of hydrogen bonding within the GTP-binding site. Other interesting results regarding the activities of the benzylamine derivatives were shown by the loss of the inhibitory activity in the case of **25**, directing attention to the importance of optimizing the length of the linker between the quinone and terminal aromatic moieties. In addition, the PLIF highlighted the binding site residues that were commonly involved in the interactions which include Ser41, Ser46 and Lys206.

Most of the alkyl or alkenyl substituted quinones (**26–33**) displayed no dynl inhibition, except **33** which was more active ($\text{IC}_{50} = 58 \pm 23 \mu\text{M}$) than the lead **1**. This promoted us to further investigate the activity of aliphatic side chain derivatives through the introduction of heteroatom bearing substituents to target more hydrogen bond interactions at the binding site. Compounds **34–43** were synthesized essentially as described in Scheme 1, using a selected library of primary amines, and subsequently screened for dynl inhibition (Table 3) [35].

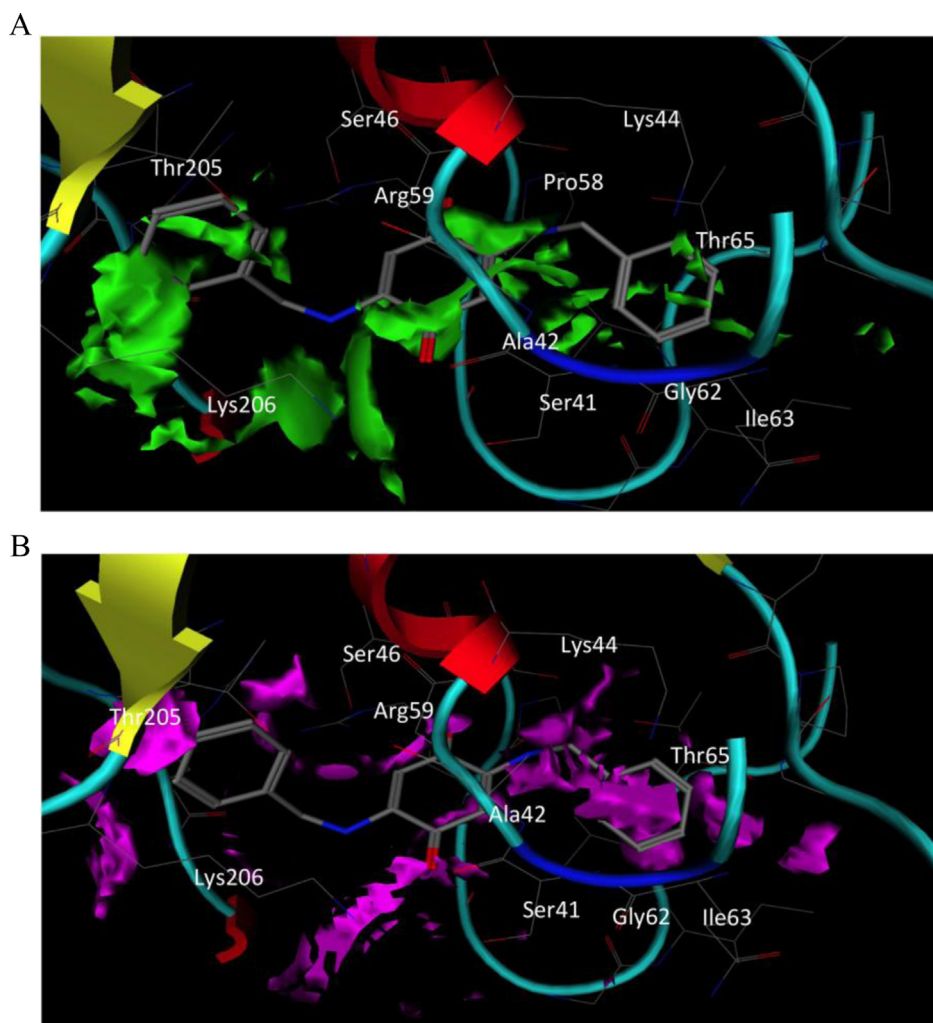
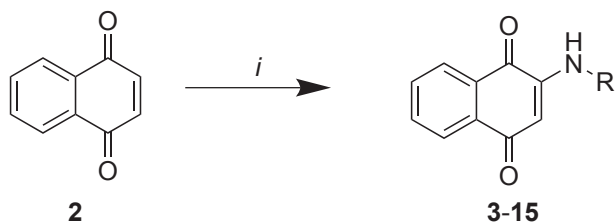


Fig. 2. Maps for contact preferences at the GTP-binding site of dynl with the docked compound **1** (sticks) showing hydrophobic favouring contacts (**A**, green) mostly near the dynamine specific loop (residues 236–246) and hydrophilic favouring interactions (**B**, purple) closer to the P-G4-loops side. (For interpretation of the references to colour in this figure legend, the reader is referred to the web version of this article.)

As was predicted from our modelling study, the introduction of a terminal –OH moiety gave moderate level of dynl inhibition with the ethyl (**34**) containing derivative returning an IC_{50} value of 116 ± 49 (Table 3). However, further chain elongation to propyl (**35**) or butyl (**36**) resulted in a complete loss of activity (dynl $IC_{50} > 300 \mu M$). Methylation of the terminal OH group (**37** and **38**) or its replacement with other heteroatoms (**39** and **40**) was generally detrimental to activity. Replacement of the bromo substituent in **33** with chloro (**41** and **43**) lead to a complete loss of activity. The same result was observed on shortening of the linker unit between the bromo and the quinone moieties (**42**). It was clear



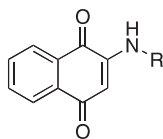
Scheme 1. Reagents and conditions: (i).

from the data obtained with the alkylamine derivatives that a hydrogen bond donating substituent with a two carbon spacer to the amino group was important for retaining dynl inhibition activity.

With only moderate enhancement in the activity observed by the omission of the peripheral phenyl moiety, we decided to retain this moiety during further structural optimization. It was also clear from the inhibitory data that hydrogen bonding interactions were crucial for inhibitor activity. To further explore this, the optimum length for the linker between the quinone core and the peripheral aromatic moiety was examined. Two molecules were designed by elongating the aminomethyl spacer in **23** to aminoethyl (**44**) and shortening it to amino (**45**) and these were subjected to modelling analysis. Both docked poses were inspected prior to the post-docking energy minimization in order to investigate possible steric clashes or unfavourable ligand orientations. The docking pose for **44** revealed an unfavourable orientation within the active site with one of the aromatic side chains clashing with GTP binding pocket residues (Fig. 4A).

Analysis of the docking pose of **45** revealed a better hydrogen bonding network with no steric clashes at the active site. The energy minimized pose of the docked **45** showed similar interactions to those observed with the parent **1**, with an essentially identical

Table 1
Inhibition of dynl PS-stimulated GTPase activity by amine substituted 1,4-naphthoquinone analogues **3–15**.



Compound	R	Dynl IC ₅₀ (μM)
3	–(CH ₂) ₂ OH	–
4	–(CH ₂) ₃ OH	–
5	Ph	–
6	2-COOH-Ph	314
7	3-COOH-Ph	–
8	4-COOH-Ph	–
9	3-CH ₂ OH-Ph	30.3 ± 5.7 ^a
10	4-CH ₂ OH-Ph	29.5 ± 5.7 ^a
11	3-OH-Ph	109
12	4-OH-Ph	22.4 ± 1.5 ^a
13	–CH ₂ Ph	–
14	–CH ₂ -4-OCH ₃ -Ph	–
15	–CH ₂ -4-OH-Ph	150

(–) not active up to 300 μM.

^a n = 3.

orientation at the active site (Fig. 5B). Both hydroxyl moieties were involved in strong backbone and side chain hydrogen bonding with different loops of the binding site. In addition, both amino groups were able to act as hydrogen bond donors generating two strong backbone interactions with Gly60 and Arg237.

Based on the predicted more favourable binding for **45**, a series of substituted aniline analogues was synthesized for screening against dynl GTPase activity (Table 4).

The data presented in Table 4 showed that the parent aniline (**46**) was devoid of activity. However, the introduction of a 2-CO₂H (**47**), 3-CO₂H (**48**) or 4-CO₂H (**49**) saw a significant increase in dynl inhibition in line with that predicted by our modelling analysis, with these compounds returning dynl IC₅₀ values of 50.2, 25.4 and 10.6 μM respectively. Polar substituents were generally best tolerated, with compounds containing hydroxyl and carboxylate substituents exhibiting the greatest inhibitory activity. The position of the aromatic substituent was found to affect the inhibition activity (**47** vs. **49**, **45** vs. **50** and **56** vs. **58**). As anticipated from modelling observations, the methyl (**51**), methoxy (**52–54**) and bromo (**55**) substituents were poorly tolerated, with IC₅₀ > 300 μM.

Molecular docking simulations revealed similarities between the binding pose of **49** and that of **45**, with **49** forming strong network of hydrogen bonding interactions with residues at the dynamin-specific loop (Supplementary data). These new interactions involved extensive hydrogen bonding between the carboxyl groups and the backbones/side chains of residues Asp208, Val234, Val235 and Asn236.

Finally, in order to confirm that these quinone based compounds target the GTP active site of dynl, a series of Michaelis Menten kinetic experiments were conducted with quinone-**58**. The Lineweaver–Burke plots revealed clear competitive inhibition with respect to Mg²⁺.GTP for dynl (Fig. 5), consistent with the modelling predictions.

2.1. Inhibition of clathrin-mediated endocytosis

The parent compound **1** as well as five quinone analogues **45** and **47–50** were quantified for their ability to inhibit the

internalization of Tfn-A594 into U2OS cells as well as dynII GTPase activity (Table 5).

The results revealed that five compounds possessed some degree of CME inhibitory activity using transferrin endocytosis, with only **50** failing to exert any effect (**50**, IC_{50(CME)}: Not Active). Compound **45** was the most potent CME inhibitor, returning an IC_{50(CME)} of 36 ± 16 μM, whilst the remaining active analogues exhibited modest (**1**, IC_{50(CME)}: 120 ± 27 μM) to weak (**48**, IC_{50(CME)}: >300 μM) levels of CME inhibitory activity.

Whilst these results could indicate differences in dyn/II inhibitory activity and specificity for one isoform, results obtained from dynII GTPase inhibition by selected compounds showed no isoform selectivity (Fig. 5). Accordingly, the differences in inhibitory activities against full length dynI versus CME were likely due to differences in the membrane permeability of each compound. We therefore calculated the polar accessible surface area (PASA) [37,38] for **1**, **45**, and **47–50** which showed values that were consistent with the apparent CME activities (Table 5). Of the six examined analogues, **1** had the lowest PASA value (107 Å²) and the smallest difference between the dynI IC₅₀ value and the CME IC₅₀ value. Conversely, **48** and **49** both possessed higher PASA values (298 and 302 Å² respectively), resulting in lower membrane permeability and up to 20-fold decrease in the CME IC₅₀ relative to the dynI IC₅₀. This was also true when comparing **49** (PASA value of 302 Å²) and **45** (PASA value of 204 Å²), where a COOH to OH substitution caused an equipotent dynI inhibitory activity, but a 5-fold improvement in CME inhibitory activity.

Differences in membrane permeability were also likely to account for the differences in CME block noted for the isomeric derivatives **47–49**. The isomer **47** (*o*-COOH) was found to exhibit the highest CME inhibitory activity of the three analogues, returning an IC_{50(CME)} of 162 ± 41 μM. Whilst this represents more than 3-fold reduction in potency compared to the dynI inhibitory activity, it was a significant improvement compared to the greater than 20-fold reduction in potency observed for **48** and **49**. Further evidence for the membrane permeability problem amongst the carboxyl containing analogues was provided through the calculation of the hydrogen bond donating capacity (HBD_{cap}) for each derivative (Table 5). The *ortho* carboxyl isomer (**47**) showed a significantly lower HBD_{cap} (304) compared to the other two isomers (**31** and **32**) which show HBD_{cap} of 399 and 479 respectively. This low HBD_{cap} for **47** was due to the positioning of the COOH moiety proximal to the NH group allowing for an intramolecular hydrogen bond formation which contributes in shielding the polarity of **47**, facilitating membrane permeability [39,40].

Despite the differences in the rank order between the CME and dynI inhibitory activities of the examined quinones, the results were consistent with the inhibition of dynI by aminoquinone compounds resulting in inhibition of CME, provided the inhibitor was both sufficiently potent against the protein target, and was cell permeable.

3. Conclusion

Herein we have reported the identification 2,5-bis(benzylamino)cyclohexa-2,5-diene-1,4-dione (**1**) as a 273 ± 106 μM potent inhibitor of dynI. This lead was identified through a virtual screening approach. Detailed docking analysis suggested a number of favourable hydrogen bonding, hydrophobic and electrostatic interactions with the binding site. Using a combination of molecular modelling led design and focused library synthesis we developed four discrete naphthoquinone (**3–15**) and *p*-benzoquinone (**17–33**; **34–43**; and **45–58**) based compound libraries.

Biological evaluation highlighted a preference for polar substituents capable of forming hydrogen bonds and/or participating

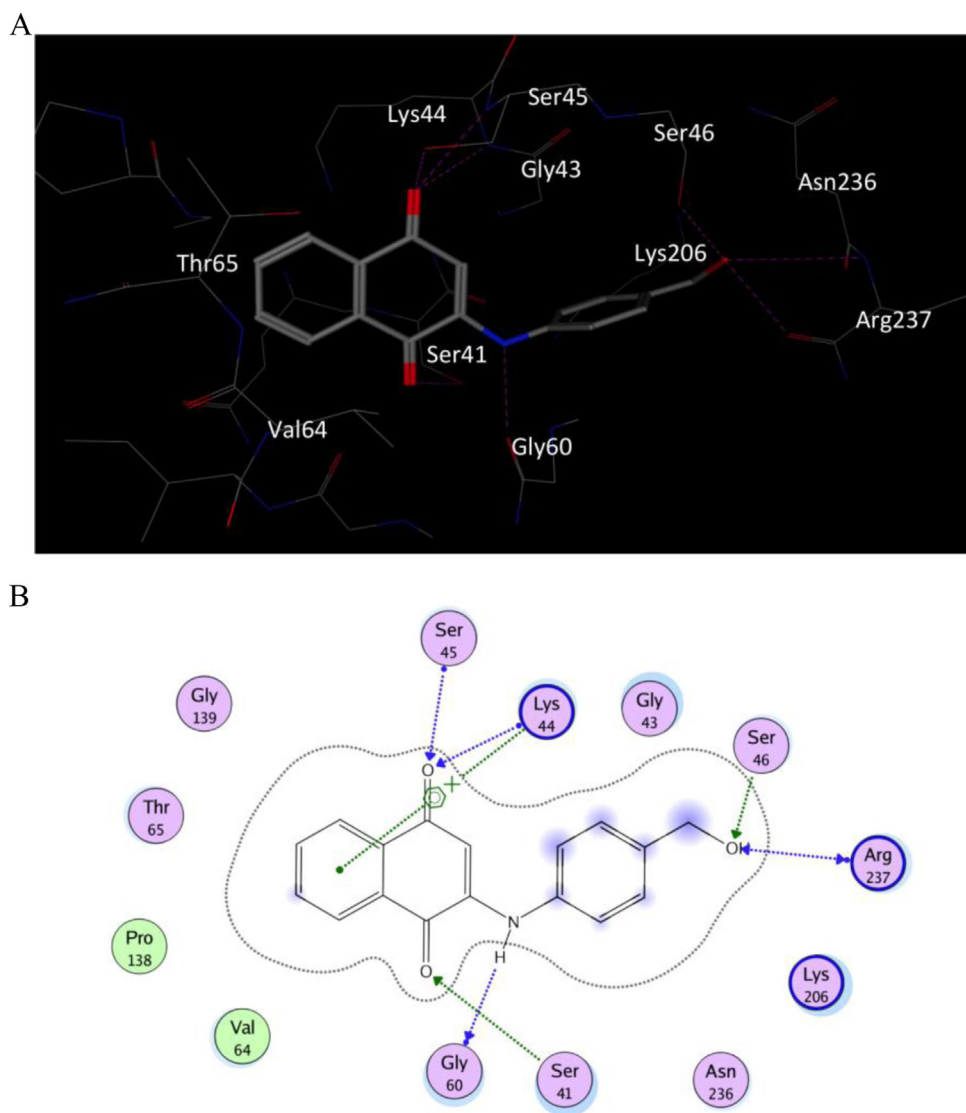


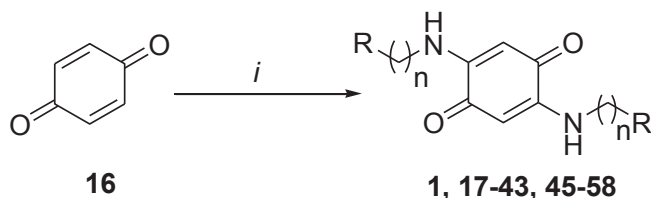
Fig. 3. **A.** Predicted binding pose of **10** in the dynI GTP-binding site. Hydrogen bonding interactions (purple dash lines) are observed with Ser41, Lys44, Ser45, Ser46, Gly60 and Arg237, whilst hydrophobic contacts are observed between the ligand and Ala42, Ile63, Val64, Leu137, Pro138 and Ile242. **B.** 2D representation for the same pose shown in **A** showing in addition the arene–cation interaction between the naphthoquinone core and the side chain of Lys44. (For interpretation of the references to colour in this figure legend, the reader is referred to the web version of this article.)

in electrostatic interactions with residues within the binding site. This was consistent with our modelling analysis. Analogues containing short-chain alcohol substituents (2 carbons) were the most potent dynI inhibitors.

A positional preference was also noted on the aromatic rings, with *para*-substituted analogues consistently exhibiting a higher potency than their positional isomers. Direct coupling to the

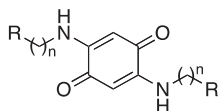
quinone moiety in the form of a substituted aniline was preferred (c.f. substituted benzylamines). Among these analogues, the *p*-hydroxy and *p*-carboxy aniline derivatives **45** and **49** with IC_{50} values of 11.1 ± 3.6 and 10.6 ± 1.6 μ M, respectively were the most potent. This represented a >20-fold activity enhancement relative to the lead, **1**. Docking studies revealed that the binding conformation of **45** and **49** in the dynI GTP-binding site is stabilized primarily by hydrogen bonding and hydrophobic interactions. The close proximity of these compounds to the G2 consensus region of the GTP-binding site leads to the suggestion that its activity may result from the compound interfering with the co-ordination of Mg^{2+} with the binding site. This was confirmed by enzyme kinetic experiments which showed quinone-**58** acted as a competitive inhibitor with respect to Mg^{2+} .GTP for dynI.

Six active analogues (**1**, **45** and **47–50**) were evaluated for their CME inhibition among which five were found to possess some degree of CME inhibitory activity. The *p*-OH substituted **45** was the most active against CME with an $IC_{50(CME)}$ of 36 ± 16 μ M consistent



Scheme 2. Reagents and conditions: (i) RNH_2 (0.5 equivalents), ethanol, reflux, 18 h.

Table 2
Inhibition of dynI PS-stimulated GTPase activity by quinone analogues **1**, **17**–**33**.



Compound	n	R	DynI IC ₅₀ (μM)
1	1	Ph	273 ± 106 ^a
17	1	3-pyridyl	–
18	1	4-COOH-Ph	29
19	1	4-CH ₃ -Ph	–
20	1	4-F-Ph	–
21	1	4-OCH ₃ Ph	170
22	1	4-Br-Ph	–
23	1	4-OH-Ph	112
24	1	4-Cl-Ph	–
25	2	Ph	–
26	1	CH ₃	–
27	2	CH ₃	–
28	3	CH ₃	–
29	4	CH ₃	–
30	5	CH ₃	>300
31	2	CH(CH ₃) ₂	–
32	1	CH=CH ₂	–
33	3	Br	58 ± 23 ^b

(–) not active up to 300 μM.

^a n = 3.

^b n = 2.

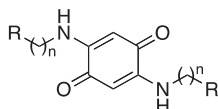
with its dynI inhibition. No isoform-selectivity was observed as the 4 compounds tested essentially equipotent against dynII. The low levels of CME inhibition observed with **47**–**49** were attributed to their low levels of predicted membrane permeability and thus reduced cellular uptake.

4. Experimental

4.1. Molecular modelling

Molecular modelling studies were performed using the crystal structure of dynI GTPase domain bound to GMPPCP ligand (PDB

Table 3
Inhibition of dynI PS-stimulated GTPase activity by quinone analogues **34**–**43**.



Compound	n	R	DynI IC ₅₀ (μM)
34	2	OH	116 ± 49 ^b
35	3	OH	– ^a
36	4	OH	–
37	2	OCH ₃	–
38	3	OCH ₃	–
39	2	SCH ₃	–
40	2	N(CH ₃) ₂	>300
41	2	Cl	– ^a
42	2	Br	–
43	3	Cl	–

(–) not active up to 300 μM.

^a n = 2.

^b n = 3.

code: 3ZYC) [3]. The pdb file was imported into Accelrys Discovery Studio package and was processed through deletion of the ligand, the water of crystallization and the co-crystallized ions. Residues at the enzyme active site that interact with the bound ligand were set as flexible residues during docking simulations. The ligand 3D structures were built using Molecular Operating Environment (MOE) software, their partial charges were assigned and energy minimized through MMFF94x force field to a gradient of 0.001, then saved as pdb files. Docking simulations were performed using AutoDock 4.2 [34] and AutoDock tools (ADT) [41] packages applying the selective receptor flexibility function. A grid map of 44 × 44 × 44 grid points, centred on the GMPPCP ligand of the complex structures, was used to cover the binding pocket. A spacing of 0.375 Å was set centred at X = 12.685; Y = 18.265; Z = –4.842 and flexible residues were set to Ser41, Lys44, Ser46 and Arg237. A Lamarckian genetic algorithm was used with the following parameters: number of individuals in population, 100; maximum number of energy evaluations, 2,500,000; maximum of generations, 27,000. Docking results were clustered with a rms tolerance of 2.0 Å. The lowest energy conformation from each cluster was taken as possible binding mode and was typed with CHARMM force field then subjected to a steepest descent energy minimization to a maximum steps of 5000 or until converged to rms gradient of 0.01. The minimized structures were investigated using MOE software for possible interactions and contacts map calculations.

Polar accessible surface area (PASA) and hydrogen bonding capacity (HBD_{cap}) were calculated using the “Descriptors” function implemented in MOE software. The 3D structures of the ligands were built using MOE builder and were energy minimized to a gradient of 0.001 using MMFF94x force field and were saved as an mdb file for descriptors calculation.

4.2. Biology

4.2.1. Materials

Phosphatidylserine (PS), phenylmethylsulfonyl fluoride (PMSF), Tween 80, fibronectin and DAPI were from Sigma Aldrich (St. Louis, MO). GTP was from Roche Applied Science (Basel, Switzerland) and leupeptin was from Bachem (Bubendorf, Switzerland). Paraformaldehyde (PFA) was from BDH (AnalaR Merck Chemicals, Darmstadt, Germany). Phosphate buffered salts, foetal bovine serum (FBS) and Dulbecco's Minimal Essential Medium (DMEM) were from Invitrogen (Paisley, Strathclyde, UK). Texas-red conjugated transferrin (Tfn-TxR), Alexa-488 conjugated EGF (EGF-A488), Alexa-594 conjugated Transferrin (Tfn-A594), DAPI and Fluo3-AM were from Molecular Probes (Eugene, OR, USA). All other reagents were of analytical reagent grade or better.

4.2.2. Compounds

Compounds were synthesized in-house and made up as 30 mM stock solutions in 100% DMSO and diluted in 50% v/v DMSO/20 mM Tris/HCl pH 7.4 or cell media prior to further dilutions in the assay. The final DMSO concentrations in the GTPase or endocytosis assays were at most 3.3% or 1% respectively. The GTPase assay for dynI was unaffected by DMSO up to 3.3% or 2.5% respectively. Stock solutions were stored at –20 °C for several months. Dynole-34-2™ was used as a positive control showing comparable activity to the previously reported data [22].

4.2.3. Protein production

Native endogenous dynI was purified from sheep brain by extraction from the peripheral membrane fraction of whole brain [13], and affinity purification on GST-Amph2-SH3-sepharose as previously described [18], yielding 8–10 mg of protein from 250 g

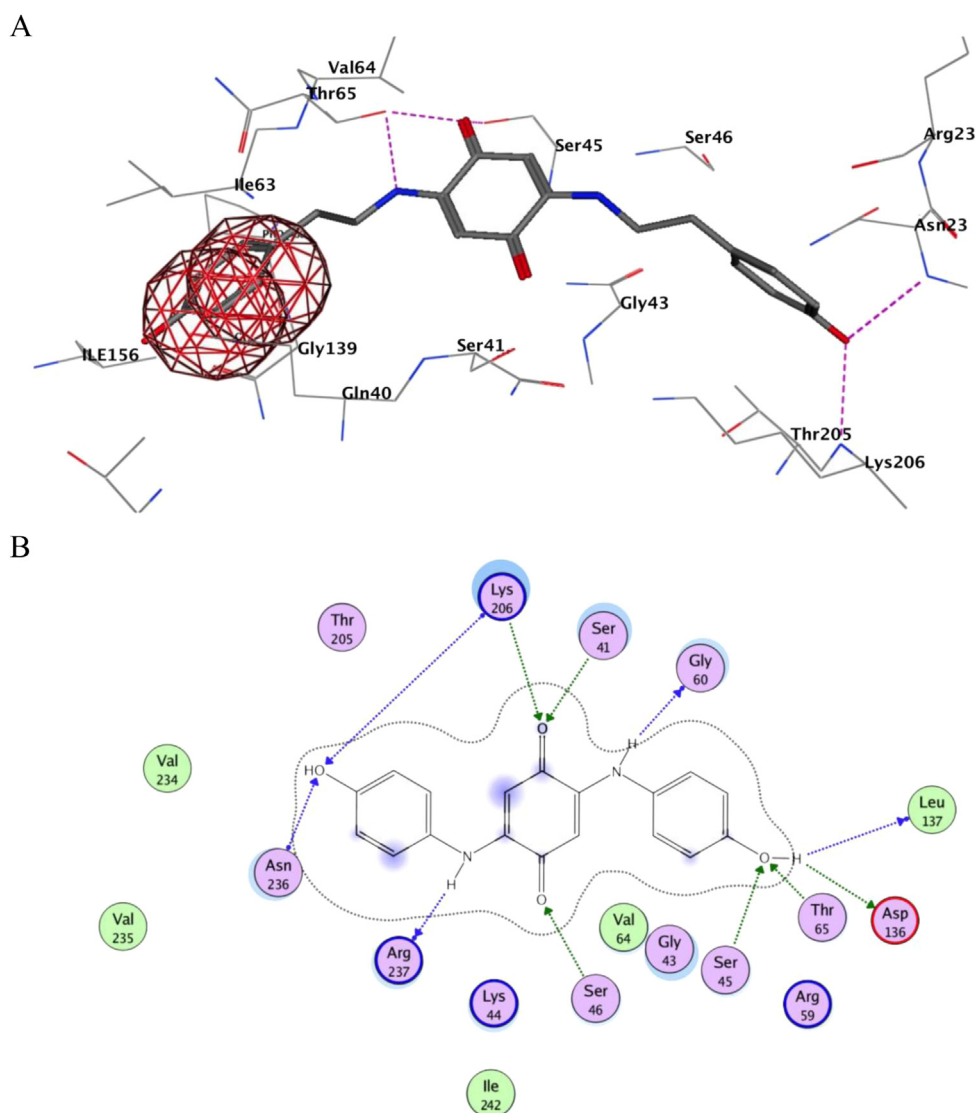


Fig. 4. A. Predicted binding pose of **44** (sticks representation) in the GTP-binding site showing steric clashes between the hydroxyphenyl moiety and residues at the active site in red line spheres. B. 2D predicted binding pose of **45** in the GTP-binding site. Hydrogen bonding interactions are observed between **45** and Ser41, Ser45, Ser46, Gly60, Thr65, Asp136, Leu137, Lys206, Asn236 and Arg237 with potential hydrophobic contacts observed with Val64 and Leu137 and Val234 (see Fig. 2 for legend). (For interpretation of the references to colour in this figure legend, the reader is referred to the web version of this article.)

of sheep brain. Recombinant rat dynamin II was expressed and purified as previously described [13]. In brief, dynII (His-6-tagged) DNA was inserted in to the pEx-6 vector and the plasmid was used to transfect Sf21 insect cells using transfection with polyethylenimine using a DNA:polyethylenimine ratio of 1:5 for 48 h. Following transfection the cells were harvested and 9 mg dynII was purified to >98% purity from 1 L of insect cell suspension culture (1×10^6 cells/mL) using GST-Amph2-SH3-sepharose as reported for dynI [13].

4.2.4. Dynamin GTPase assay

The Malachite Green method was used for the sensitive colorimetric detection of orthophosphate (P_i) release from GTP as previously described [17]. DynI or dynII (each at 50 nM in the reaction) activity was stimulated by phosphatidylserine (PS) liposomes for 30 (dynI) or 90 (dynII) minutes. Data analysis and enzyme kinetics using non-linear regression was performed using Prism 5 (GraphPad Software Inc., San Diego, CA).

4.2.5. CME assay

CME was examined by quantifying the uptake of Alexa-495-conjugated transferrin (Tfn-A495) in serum-starved U2OS cells using methods described previously [22]. Briefly, cells were plated on fibronectin-coated 96-well glass-bottomed plate to 70–80% confluency, then serum-starved overnight (16 h). Cells were pre-incubated with test compounds or vehicle (1% DMSO) for 30 min prior to the addition of 4 μ g/mL Tfn-A495 for 8 min at 37 °C. Surface-bound Tfn was removed with an ice-cold acid wash solution (0.2 M acetic acid, 0.5 M NaCl, pH 2.8) for 15 min followed by an ice-cold PBS wash for 5 min. Cells were immediately fixed with 4% PFA for 10 min at room temperature. Nuclei were stained using DAPI. Quantitative analysis of Tfn-A594 uptake in U2OS cells was performed by high content imaging. Nine images were collected from each well, averaging 40–50 cells per image. The average integrated intensity of Tfn-A594 signal per cell was calculated for each well using MetaXpress (Molecular Devices), and the data expressed as a percentage of control cells (vehicle treated only).

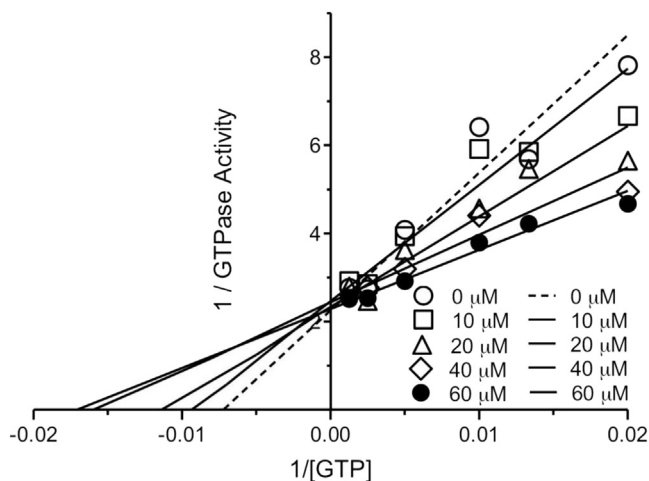


Fig. 5. Competitive kinetics of quinone-58 with respect to Mg^{2+} -GTP. The data depicts quinone-58 concentration dependent changes in double-reciprocal plot between substrate (GTP at 60–200 μM) and reaction velocity (V). The data corresponds to quinone-58 concentrations of 30 (\bullet), 20 (\diamond), 12 (Δ), and 8 (\square) μM . Error bars represent mean \pm SEM of four independent experiments each conducted in triplicate.

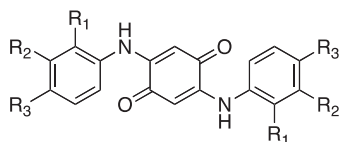
IC_{50} values were calculated using Graphpad Prism 5 and data was expressed as mean 95% confidence interval (CI) for 3 wells and ~ 1200 cells.

4.3. Chemistry

4.3.1. General methods

All reactions were performed using standard laboratory equipment and glassware. Solvents and reagents were purchased from Sigma Aldrich, Lancaster International or TCI and used as received. Organic solvents were bulk quality, and were distilled from glass prior to use. Organic solvent extracts were dried with magnesium sulfate ($MgSO_4$), and dried under reduced pressure with either

Table 4
Inhibition of dyn1 PS-stimulated GTPase activity by substituted aniline analogues 45–58.



Compound	R ₁	R ₂	R ₃	Dyn1 IC_{50} (μM)
45	H	H	OH	11.1 \pm 3.6 ^b
46	H	H	H	–
47	COOH	H	H	50.2 \pm 14.4 ^b
48	H	COOH	H	25.4 \pm 11.3 ^b
49	H	H	COOH	10.6 \pm 1.6 ^a
50	H	OH	H	57.9 \pm 17.2 ^b
51	H	H	CH ₃	–
52	OCH ₃	H	H	–
53	H	OCH ₃	H	>300
54	H	H	OCH ₃	>300
55	Br	H	H	387
56	CH ₂ OH	H	H	>>300
57	H	CH ₂ OH	H	–
58	H	H	CH ₂ OH	21.5 \pm 3.1 ^a

(–) not active up to 300 μM .

^a n = 2.

^b n = 3.

Büchi or Heidolph rotary evaporators. Melting points were recorded in open capillaries on a Stuart SMP11 Melting Point Apparatus. Temperatures are expressed in degrees Celsius ($^{\circ}C$) and are uncorrected. Where available, literature values are provided and appropriately referenced. Electrospray mass spectra were recorded using 10% DMSO/ H_2O or HPLC-grade methanol or acetonitrile as carrier solvents on a Shimadzu LC–MS spectrometer.

Nuclear magnetic resonance (NMR) spectroscopy was performed on a Bruker Avance 300 MHz spectrometer, where proton NMR (1H NMR) spectra and carbon NMR (^{13}C NMR) spectra were acquired at 300 and 75 MHz respectively, or a Bruker Avance III 400 MHz spectrometer, where 1H NMR and ^{13}C NMR were acquired at 400 and 100 MHz respectively. All spectra were recorded in deuterated dimethyl sulfoxide ($DMSO-d_6$), obtained from Sigma Aldrich or Cambridge Isotope Laboratories Inc., unless otherwise stated, with the residual solvent peaks used as the internal reference (δ 2.49 (quintet) and δ 39.7 (septet) for 1H NMR and ^{13}C NMR respectively). Chemical shifts (δ) were measured in parts per million (ppm) and referenced against the internal reference peaks. Coupling constants (J) were measured in Hertz (Hz).

NMR assignments were determined through the interpretation of one- and two-dimensional spectra, specifically gradient heteronuclear single quantum correlation (gHSQC), gradient heteronuclear multiple bond correlation (gHMBC) and distortionless enhancement by polarization transfer quaternary (DEPTQ) spectroscopy. Multiplicities are denoted as singlet (s), broad singlet (br s), doublet (d), doublet of doublets (dd), doublet of doublet of doublets (ddd), triplet (t), triplet of doublets (td), doublet of triplets (dt), quartet (q), quintet (quin) and multiplet (m). Peaks are listed in increasing chemical shift in the following format: chemical shift (integration (1H), multiplicity (1H), coupling constant (1H)).

4.3.2. General procedure for the synthesis of 2,5-bis(benzylamino)-1,4-benzoquinone (1)

To a stirred solution of 1,4-benzoquinone (0.403 g, 3.73 mmol) in ethanol (5 mL), was added a solution of benzylamine (0.224 g, 2.41 mmol) in ethanol (5 mL). The resulting dark red solution was stirred at reflux for 18 h. The obtained mixture was allowed to cool to room temperature, then kept at 4 $^{\circ}C$ for 24 h. The precipitate was washed sequentially with ethanol and ether, and dried under vacuum to afford the desired compound as an orange-red solid. Yield 0.088 g (47%); mp 229–230 $^{\circ}C$ (Lit. 252 $^{\circ}C$; 234 $^{\circ}C$; 259 $^{\circ}C$; 259 $^{\circ}C$; 253 $^{\circ}C$) [42].

1H NMR ($DMSO-d_6$) δ 4.35 (4H, d, J = 6.6 Hz), 5.16 (2H, s), 7.27 (10H, m), 8.30 (2H, t, J = 6.6 Hz, NH).

^{13}C NMR ($DMSO-d_6$) δ 45.3, 93.4, 127.3, 127.4, 128.6, 137.5, 151.1, 177.9.

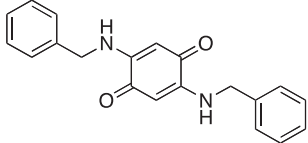
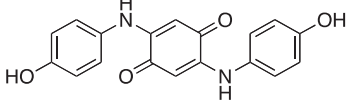
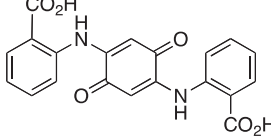
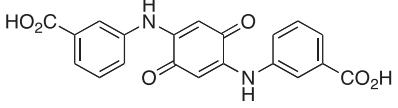
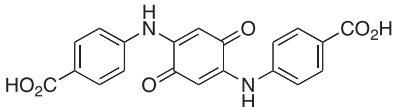
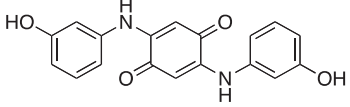
MS (ESI+) m/z : 319 (M+H), HRMS (ESI+) m/z calculated for $C_{20}H_{18}N_2O_2$ (M+H) 319.1447; found 319.1441.

4.3.3. General procedure for the synthesis of 2-(2-hydroxyethylamino)-1,4-naphthoquinone (3)

To a stirred suspension of 1,4-naphthoquinone (0.328 g, 2.07 mmol) in methanol (8 mL) was added ethanolamine (0.104 g, 1.70 mmol). The resulting dark red solution was stirred at 25 $^{\circ}C$ for 18 h. The obtained mixture was poured into cold water (40 mL), and the resulting orange-brown suspension was stirred at 25 $^{\circ}C$ for 30 min. The mixture was kept at 4 $^{\circ}C$ overnight. The precipitate was collected by filtration, washed with ice-cold water, and dried under vacuum to afford the desired compound as a red-brown solid. Yield 0.125 g (37%); mp 146–147 $^{\circ}C$ (Lit. 159–160 $^{\circ}C$) [43].

1H NMR ($DMSO-d_6$) δ 3.23 (2H, q, J = 6.0 Hz), 3.59 (2H, t, J = 6.0 Hz), 4.85 (1H, br s, OH), 5.72 (1H, s), 7.28 (1H, t, J = 6.0 Hz, NH), 7.71 (1H, td, J = 1.5, 7.5 Hz), 7.81 (1H, td, J = 1.5, 7.5 Hz), 7.93 (1H, dd, J = 1.5, 7.5 Hz), 7.97 (1H, dd, J = 1.5, 7.5 Hz).

Table 5
CME inhibition data for quinone based dynamin inhibitors, compared with *in vitro* dyn GTPase activity inhibition.

Compound	Structure	DynI IC ₅₀ (μM)	DynII IC ₅₀ (μM)	CME IC ₅₀ (μM)	PASA ^a	HBD_cap ^b
1		273	–	120 ± 27	107	193
45		11.1 ± 3.6 ^f	23.6	36 ± 16	204	329
47		50.2 ± 14.4 ^f	ND ^c	162 ± 41	243	304
48		25.4 ± 11.3 ^e	14.7	>300	298	399
49		10.6 ± 1.6 ^e	9.1	200 ± 41	302	479
50		57.9 ± 17.2 ^f	43.7	–	NC ^d	NC ^d

(–) Not active up to 300 μM.

^a Polar accessible surface area (Å²).

^b Hydrogen bond donor capacity.

^c Not determined.

^d Not calculated.

^e *n* = 2.

^f *n* = 3.

¹³C NMR (DMSO-*d*₆) δ 44.8, 58.6, 99.8, 125.5, 126.1, 130.5, 132.4, 133.3, 135.0, 148.9, 181.5, 181.7.

MS (ESI+) *m/z*: 218 (M+H), HRMS (ESI+) *m/z* calculated for C₁₂H₁₁NO₃ (M+H) 218.0817; found 218.0812.

4.3.4. 2-(3-Hydroxypropylamino)-1,4-naphthoquinone (4)

Synthesized using the same general procedure described for the synthesis of **3**, commencing with 1,4-naphthoquinone and 3-amino-1-propanol to afford the title compound as an orange-brown solid. Yield 0.158 g (40%); mp 120–121 °C.

¹H NMR (DMSO-*d*₆) δ 1.73 (2H, m), 3.23 (2H, m), 3.49 (2H, m), 4.61 (1H, t, *J* = 5.1 Hz, OH), 5.67 (1H, s), 7.53 (1H, t, *J* = 6.0 Hz, NH), 7.70 (1H, td, *J* = 1.5, 7.5 Hz), 7.81 (1H, td, *J* = 1.5, 7.5 Hz), 7.93 (1H, dd, *J* = 1.5, 7.5 Hz), 7.96 (1H, dd, *J* = 1.5, 7.5 Hz).

¹³C NMR (DMSO-*d*₆) δ 30.6, 39.8, 58.9, 99.4, 125.5, 126.0, 130.6, 132.3, 133.4, 135.0, 148.7, 181.4, 181.7.

MS (ESI+) *m/z*: 232 (M+H), HRMS (ESI+) *m/z* calculated for C₁₃H₁₃NO₃ (M+H) 232.0974; found 232.0968.

4.3.5. 2-(Anilino)-1,4-naphthoquinone (5)

Synthesized using the same general procedure described for the synthesis of **3**, commencing with 1,4-naphthoquinone and aniline to afford the title compound as a dark red solid. Yield 0.209 g (49%); mp 185 °C (Lit. 191–192 °C) [44].

¹H NMR (DMSO-*d*₆) δ 6.09 (1H, s), 7.21 (1H, m), 7.41 (4H, m), 7.77 (1H, td, *J* = 1.5, 7.5 Hz), 7.85 (1H, td, *J* = 1.5, 7.5 Hz), 7.94 (1H, dd, *J* = 1.5, 7.5 Hz), 8.05 (1H, dd, *J* = 1.5, 7.5 Hz), 9.21 (1H, br s, NH).

¹³C NMR (DMSO-*d*₆) δ 102.1, 123.9 (2C), 125.5 (2C), 126.3, 129.5 (2C), 130.6, 132.8 (2C), 135.1, 138.3, 146.4, 181.8, 182.8.

MS (ESI+) *m/z*: 250 (M+H), HRMS (ESI+) *m/z* calculated for C₁₆H₁₁NO₂ (M+H) 250.0868; found 250.0863.

4.3.6. 2-(2-Carboxyanilino)-1,4-naphthoquinone (6)

Synthesized using the same general procedure described for the synthesis of **3**, commencing with 1,4-naphthoquinone and anthranilic acid to afford the title compound as an orange-red solid. Yield 0.156 g (56%); mp > 250 °C (Lit. 237–240 °C (dec.)) [44].

¹H NMR (DMSO-*d*₆) δ 6.56 (1H, s), 7.22 (1H, m), 7.68 (2H, m), 7.81 (1H, td, *J* = 1.8, 7.5 Hz), 7.88 (1H, td, *J* = 1.8, 7.5 Hz), 7.97 (1H, dd, *J* = 1.8, 7.5 Hz), 8.03 (1H, m), 8.08 (1H, dd, *J* = 1.8, 7.5 Hz), 10.82 (1H, br s, NH).

¹³C NMR (DMSO-*d*₆) δ 105.2, 120.0, 120.8, 123.5, 125.6, 126.6, 130.5, 132.2, 132.5, 133.2, 134.3, 135.2, 140.3, 143.9, 169.0, 181.6, 183.5.

MS (ESI⁻) *m/z*: 292 (M⁻H), HRMS (ESI⁻) *m/z* calculated for C₁₇H₁₁NO₄ (M⁻H) 292.0610; found 292.0615.

4.3.7. 2-(3-Carboxyanilino)-1,4-naphthoquinone (7)

Synthesized using the same general procedure described for the synthesis of **3**, commencing with 1,4-naphthoquinone and 3-aminobenzoic acid to afford the title compound as a dark red solid. Yield 0.239 g (64%); mp > 250 °C (Lit. 264–265 °C) [44].

¹H NMR (DMSO-*d*₆) δ 6.12 (1H, s), 7.55 (1H, t, *J* = 7.8 Hz), 7.64 (1H, m), 7.76 (1H, m), 7.79 (1H, td, *J* = 1.5, 7.5 Hz), 7.86 (1H, td, *J* = 1.5, 7.5 Hz), 7.92 (1H, d, *J* = 1.8 Hz), 7.95 (1H, dd, *J* = 1.5, 7.5 Hz), 8.07 (1H, dd, *J* = 1.5, 7.5 Hz), 9.34 (1H, br s, NH), 13.15 (1H, br s, COOH).

¹³C NMR (100 MHz) (DMSO-*d*₆) δ 102.5, 124.2, 125.5, 126.0, 126.3, 128.1, 129.8, 130.6, 132.1, 132.7, 132.9, 135.1, 138.7, 146.3, 167.0, 181.6, 182.9.

MS (ESI⁻) *m/z*: 292 (M⁻H), HRMS (ESI⁻) *m/z* calculated for C₁₇H₁₁NO₄ (M⁻H) 292.0610; found 292.0615.

4.3.8. 2-(4-Carboxyanilino)-1,4-naphthoquinone (8)

Synthesized using the same general procedure described for the synthesis of **3**, commencing with 1,4-naphthoquinone and 4-aminobenzoic acid to afford the title compound as a dark red solid. Yield 0.148 g (40%); mp > 250 °C (Lit. 319–321 °C) [44].

¹H NMR (DMSO-*d*₆) δ 6.35 (1H, s), 7.52 (2H, d, *J* = 8.7 Hz), 7.80 (1H, td, *J* = 1.5, 7.5 Hz), 7.87 (1H, td, *J* = 1.5, 7.5 Hz), 7.96 (1H, dd, *J* = 1.5, 7.5 Hz), 7.97 (2H, d, *J* = 8.7 Hz), 8.07 (1H, dd, *J* = 1.5, 7.5 Hz), 9.38 (1H, br s, NH).

¹³C NMR (DMSO-*d*₆) δ 104.3, 122.6, 125.7, 126.6, 126.8, 130.7, 131.0, 132.7, 133.3, 135.4, 142.9, 145.5, 167.2, 181.7, 183.5.

MS (ESI⁻) *m/z*: 292 (M⁻H), HRMS (ESI⁻) *m/z* calculated for C₁₇H₁₁NO₄ (M⁻H) 292.0610; found 292.0616.

4.3.9. 2-(3-(Hydroxymethyl)anilino)-1,4-naphthoquinone (9)

Synthesized using the same general procedure described for the synthesis of **1**, commencing with 1,4-naphthoquinone and 3-aminobenzylalcohol to afford the title compound as a maroon solid. Yield 0.243 g (52%); mp 186–187 °C.

¹H NMR (DMSO-*d*₆) δ 4.52 (2H, d, *J* = 5.7 Hz), 5.27 (1H, t, *J* = 5.7 Hz, OH), 6.11 (1H, s), 7.15 (1H, d, *J* = 7.8 Hz), 7.23 (1H, dd, *J* = 2.4, 7.8 Hz), 7.34 (1H, d, *J* = 2.4 Hz), 7.38 (1H, t, *J* = 7.8 Hz), 7.71 (1H, td, *J* = 1.5, 7.5 Hz), 7.85 (1H, td, *J* = 1.5, 7.5 Hz), 7.94 (1H, dd, *J* = 1.5, 7.5 Hz), 8.06 (1H, dd, *J* = 1.5, 7.5 Hz), 9.19 (1H, br s, NH).

¹³C NMR (DMSO-*d*₆) δ 62.7, 102.1, 121.5, 122.3, 123.5, 125.4, 126.3, 129.2, 130.6, 132.7, 135.0, 138.1, 144.1, 146.4, 181.7, 182.7.

MS (ESI⁺) *m/z*: 280 (M+H), HRMS (ESI⁺) *m/z* calculated for C₁₇H₁₃NO₃ (M+H) 280.0974; found 280.0968.

4.3.10. 2-(4-(Hydroxymethyl)anilino)-1,4-naphthoquinone (10)

Synthesized using the same general procedure described for the synthesis of **3**, commencing with 1,4-naphthoquinone and 4-aminobenzylalcohol to afford the title compound as a maroon solid. Yield 0.234 g (49%); mp 212 °C.

¹H NMR (DMSO-*d*₆) δ 4.49 (2H, d, *J* = 5.7 Hz), 5.19 (1H, t, *J* = 5.7 Hz, OH), 6.06 (1H, s), 7.32 (2H, d, *J* = 8.7 Hz), 7.38 (2H, d, *J* = 8.7 Hz), 7.77 (1H, td, *J* = 1.5, 7.5 Hz), 7.85 (1H, td, *J* = 1.5, 7.5 Hz), 7.94 (1H, dd, *J* = 1.5, 7.5 Hz), 8.05 (1H, dd, *J* = 1.5, 7.5 Hz), 9.20 (1H, br s, NH).

¹³C NMR (100 MHz) (DMSO-*d*₆) δ 62.7, 101.9, 123.7, 125.4, 126.3, 127.5, 130.6, 132.8, 135.1, 136.7, 139.9, 146.5, 181.8, 182.6.

MS (ESI⁺) *m/z*: 280 (M+H), HRMS (ESI⁺) *m/z* calculated for C₁₇H₁₃NO₃ (M+H) 280.0974; found 280.0978.

4.3.11. 2-(3-Hydroxyanilino)-1,4-naphthoquinone (11)

Synthesized using the same general procedure described for the synthesis of **3**, commencing with 1,4-naphthoquinone and 3-aminophenol to afford the title compound as a dark brown solid. Yield 0.250 g (53%); mp > 250 °C (Lit. 242 °C) [45].

¹H NMR (DMSO-*d*₆) δ 6.14 (1H, m), 6.61 (1H, m), 6.79 (1H, d, *J* = 1.8 Hz), 6.80 (1H, m), 7.21 (1H, t, *J* = 8.4 Hz), 7.71 (1H, td, *J* = 1.5, 7.5 Hz), 7.85 (1H, td, *J* = 1.5, 7.5 Hz), 7.94 (1H, dd, *J* = 1.5, 7.5 Hz), 8.05 (1H, dd, *J* = 1.5, 7.5 Hz), 9.08 (1H, br s, NH), 9.62 (1H, br s, OH).

¹³C NMR (100 MHz) (DMSO-*d*₆) δ 102.4, 110.5, 112.6, 114.4, 125.4, 126.3, 130.2, 130.6, 132.8 (2C), 135.0, 139.3, 146.2, 158.2, 181.7, 182.7.

MS (ESI⁺) *m/z*: 266 (M+H), HRMS (ESI⁺) *m/z* calculated for C₁₆H₁₁NO₃ (M+H) 266.0817; found 266.0812.

4.3.12. 2-(4-Hydroxyanilino)-1,4-naphthoquinone (12)

Synthesized using the same general procedure described for the synthesis of **3**, commencing with 1,4-naphthoquinone and 4-aminophenol to afford the title compound as a dark brown solid. Yield 0.341 g (76%); mp > 250 °C (Lit. 225 °C) [45].

¹H NMR (DMSO-*d*₆) δ 5.86 (1H, s), 6.82 (2H, d, *J* = 8.7 Hz), 7.15 (2H, d, *J* = 8.7 Hz), 7.75 (1H, td, *J* = 1.5, 7.5 Hz), 7.83 (1H, td, *J* = 1.5, 7.5 Hz), 7.93 (1H, dd, *J* = 1.5, 7.5 Hz), 8.03 (1H, dd, *J* = 1.5, 7.5 Hz), 9.04 (1H, br s, NH), 9.56 (1H, br s, OH).

¹³C NMR (DMSO-*d*₆) δ 101.0, 116.0, 125.4, 126.0, 126.2, 129.1, 130.6, 132.6, 133.0, 135.0, 147.2, 155.5, 181.9, 182.3.

MS (ESI⁺) *m/z*: 266 (M+H), HRMS (ESI⁺) *m/z* calculated for C₁₆H₁₁NO₃ (M+H) 266.0817; found 266.0812.

4.3.13. 2-(Benzylamino)-1,4-naphthoquinone (13)

Synthesized using the same general procedure described for the synthesis of **3**, commencing with 1,4-naphthoquinone and benzylamine to afford the title compound as an orange-brown solid. Yield 0.235 g (56%); mp 154–155 °C (Lit. 154.7–155.7 °C; 155 °C) [44].

¹H NMR (DMSO-*d*₆) δ 4.44 (2H, d, *J* = 6.6 Hz), 5.55 (1H, s), 7.27 (5H, m), 7.71 (1H, td, *J* = 1.5, 7.5 Hz), 7.80 (1H, td, *J* = 1.5, 7.5 Hz), 7.89 (1H, dd, *J* = 1.5, 7.5 Hz), 7.99 (1H, dd, *J* = 1.5, 7.5 Hz), 8.15 (1H, t, *J* = 6.6 Hz, NH).

¹³C NMR (DMSO-*d*₆) δ 45.3, 100.6, 125.5, 126.1, 127.3 (3C), 128.7 (2C), 130.6, 132.4, 133.2, 135.0, 137.6, 148.7, 181.6, 181.8.

MS (ESI⁺) *m/z*: 264 (M+H), HRMS (ESI⁺) *m/z* calculated for C₁₇H₁₃NO₂ (M+H) 264.1025; found 264.1019.

4.3.14. 2-(4-Methoxybenzylamino)-1,4-naphthoquinone (14)

Synthesized using the same general procedure described for the synthesis of **3**, commencing with 1,4-naphthoquinone and 4-methoxybenzylamine to afford the title compound as a red-brown solid. Yield 0.250 g (45%); mp 159–160 °C.

¹H NMR (DMSO-*d*₆) δ 3.71 (3H, s), 4.35 (2H, d, *J* = 6.3 Hz), 5.57 (1H, s), 6.89 (2H, d, *J* = 8.7 Hz), 7.27 (2H, d, *J* = 8.7 Hz), 7.71 (1H, td, *J* = 1.5, 7.5 Hz), 7.80 (1H, td, *J* = 1.5, 7.5 Hz), 7.89 (1H, dd, *J* = 1.5, 7.5 Hz), 7.98 (1H, dd, *J* = 1.5, 7.5 Hz), 8.09 (1H, t, *J* = 6.3 Hz, NH).

¹³C NMR (DMSO-*d*₆) δ 44.7, 55.2, 100.5, 114.1, 125.5, 126.0, 128.6, 129.3, 130.6, 132.4, 133.2, 135.0, 148.5, 158.6, 181.5, 181.8.

MS (ESI+) m/z : 294 (M+H), HRMS (ESI+) m/z calculated for $C_{18}H_{15}NO_3$ (M+H) 294.1130; found 294.1125.

4.3.15. 2-(4-Hydroxybenzylamino)-1,4-naphthoquinone (15)

Synthesized using the same general procedure described for the synthesis of **3**, commencing with 1,4-naphthoquinone and 4-hydroxybenzylamine to afford the title compound as a maroon solid. Yield 0.219 g (46%); mp 222–223 °C.

1H NMR (DMSO- d_6) δ 4.30 (2H, d, J = 6.6 Hz), 5.58 (1H, s), 6.71 (2H, d, J = 8.7 Hz), 7.14 (2H, d, J = 8.7 Hz), 7.70 (1H, td, J = 1.5, 7.5 Hz), 7.80 (1H, td, J = 1.5, 7.5 Hz), 7.89 (1H, dd, J = 1.5, 7.5 Hz), 7.97 (1H, dd, J = 1.5, 7.5 Hz), 8.03 (1H, t, J = 6.6 Hz, NH), 9.30 (1H, br s, OH).

^{13}C NMR (DMSO- d_6) δ 44.9, 100.5, 115.4 (2C), 125.5, 126.0, 127.5, 128.7 (1C), 130.6, 132.3, 133.2, 135.0, 148.5, 156.7, 181.5, 181.8.

MS (ESI+) m/z : 280 (M+H), HRMS (ESI+) m/z calculated for $C_{17}H_{13}NO_3$ (M+H) 280.0974; found 280.0968.

4.3.16. 2,5-Bis(3-pyridylmethylamino)-1,4-benzoquinone (17)

Synthesized using the same general procedure described for the synthesis of **1**, commencing with 1,4-benzoquinone and 3-(aminomethyl)pyridine to afford the title compound as an orange-brown solid. Yield 0.367 g (67%); mp 222–223 °C.

1H NMR (DMSO- d_6) δ 4.40 (4H, d, J = 6.6 Hz), 5.25 (2H, s), 7.34 (2H, dd, J = 4.8, 7.8 Hz), 7.68 (2H, dt, J = 1.8, 7.8 Hz), 8.30 (2H, t, J = 6.6 Hz, NH), 8.45 (2H, dd, J = 1.8, 4.8 Hz), 8.52 (2H, d, J = 1.8 Hz).

^{13}C NMR (100 MHz) (DMSO- d_6) δ 42.8 (2C), 93.5 (2C), 123.8 (2C), 133.2 (2C), 135.2 (2C), 148.6 (2C), 149.0 (2C), 150.9 (2C), 178.1 (2C).

MS (ESI+) m/z : 321 (M+H), HRMS (ESI+) m/z calculated for $C_{18}H_{16}N_4O_2$ (M+H) 321.1352; found 321.1346.

4.3.17. 2,5-Bis(4-carboxybenzylamino)-1,4-benzoquinone (18)

Synthesized using the same general procedure described for the synthesis of **1**, commencing with 1,4-benzoquinone and 4-(aminomethyl)benzoic acid to afford the title compound as a maroon solid. Yield 0.227 g (60%); mp > 250 °C.

1H NMR (DMSO- d_6) δ 4.44 (4H, d, J = 6.6 Hz), 5.15 (2H, s), 7.38 (4H, d, J = 8.4 Hz), 7.89 (4H, d, J = 8.4 Hz), 8.33 (2H, t, J = 6.6 Hz, NH).

^{13}C NMR (DMSO- d_6) δ 45.1 (2C), 93.7 (2C), 127.4 (4C), 129.8 (4C), 130.0 (2C), 142.8 (2C), 151.1 (2C), 167.4 (2C), 178.1 (2C).

MS (ESI-) m/z : 405 (M-H), HRMS (ESI-) m/z calculated for $C_{22}H_{18}N_2O_6$ (M-H) 405.1087; found 405.1092.

4.3.18. 2,5-Bis(4-methylbenzylamino)-1,4-benzoquinone (19)

Synthesized using the same general procedure described for the synthesis of **1**, commencing with 1,4-benzoquinone and 4-methylbenzylamine to afford the title compound as a pink-brown solid. Yield 0.262 g (64%); mp 238–240 °C.

1H NMR (DMSO- d_6) δ 2.25 (6H, s), 4.30 (4H, d, J = 6.6 Hz), 5.14 (2H, s), 7.13 (8H, m), 8.21 (2H, t, J = 6.6 Hz, NH).

^{13}C NMR (DMSO- d_6) δ 20.8 (2C), 45.1 (2C), 93.4 (2C), 127.2 (4C), 129.3 (4C), 134.4 (2C), 136.4 (2C), 151.1 (2C), 178.0 (2C).

MS (ESI+) m/z : 347 (M+H), HRMS (ESI+) m/z calculated for $C_{22}H_{22}N_2O_2$ (M+H) 347.1760; found 347.1754.

4.3.19. 2,5-Bis(4-fluorobenzylamino)-1,4-benzoquinone (20)

Synthesized using the same general procedure described for the synthesis of **1**, commencing with 1,4-benzoquinone and 4-fluorobenzylamine to afford the title compound as an orange-brown solid. Yield 0.283 g (61%); mp 229–230 °C.

1H NMR (DMSO- d_6) δ 4.34 (4H, d, J = 6.6 Hz), 5.19 (2H, s), 7.14 (4H, t, J = 8.7 Hz), 7.33 (4H, dd, J = 5.4, 8.7 Hz), 8.26 (2H, t, J = 6.6 Hz, NH).

^{13}C NMR (DMSO- d_6) δ 44.5 (2C), 93.4 (2C), 115.4 ($^2J_{CF}$ = 21.4 Hz, C_4 , C_4' , C_6 , C_6'), 129.4 ($^3J_{CF}$ = 8.1 Hz, C_3 , C_3' , C_7 , C_7'), 133.7

($^4J_{CF}$ = 2.6 Hz, C_2 , C_2'), 150.9 (2C₂), 161.5 ($^1J_{CF}$ = 242.9 Hz, C_5 , C_5'), 178.0 (2C).

MS (ESI+) m/z : 355 (M+H), HRMS (ESI+) m/z calculated for $C_{20}H_{16}F_2N_2O_2$ (M+H) 355.1258; found 355.1253.

4.3.20. 2,5-Bis(4-methoxybenzylamino)-1,4-benzoquinone (21)

Synthesized using the same general procedure described for the synthesis of **1**, commencing with 1,4-benzoquinone and 4-methoxybenzylamine to afford the title compound as a dark brown solid. Yield 0.485 g (67%); mp 222 °C.

1H NMR (DMSO- d_6) δ 3.71 (6H, s), 4.27 (4H, d, J = 6.6 Hz), 5.17 (2H, s), 6.87 (4H, d, J = 8.7 Hz), 7.21 (4H, d, J = 8.7 Hz), 8.19 (2H, t, J = 6.6 Hz, NH).

^{13}C NMR (DMSO- d_6) δ 44.7 (2C), 55.2 (2C), 93.2 (2C), 114.1 (4C), 128.5 (4C), 129.3 (2C), 151.0 (2C), 158.6 (2C), 177.9 (2C).

MS (ESI+) m/z : 379 (M+H), HRMS (ESI+) m/z calculated for $C_{22}H_{22}N_2O_4$ (M+H) 379.1658; found 379.1652.

4.3.21. 2,5-Bis(4-bromobenzylamino)-1,4-benzoquinone (22)

Synthesized using the same general procedure described for the synthesis of **1**, commencing with 1,4-benzoquinone and 4-bromobenzylamine to afford the title compound as a brown solid. Yield 0.342 g (73%); mp 186–188 °C.

1H NMR (DMSO- d_6) δ 4.33 (4H, d, J = 6.6 Hz), 5.15 (2H, s), 7.24 (4H, d, J = 8.4 Hz), 7.51 (4H, d, J = 8.4 Hz), 8.29 (2H, t, J = 6.6 Hz, NH).

^{13}C NMR (DMSO- d_6) δ 44.6 (2C), 93.6 (2C), 120.4 (2C), 129.6 (4C), 131.5 (4C), 137.1 (2C), 150.9 (2C), 178.0 (2C).

MS (ESI+) m/z : 475 (M+H), HRMS (ESI+) m/z calculated for $C_{20}H_{16}Br_2N_2O_2$ (M+H) 474.9657; found 474.9651.

4.3.22. 2,5-Bis(4-hydroxybenzylamino)-1,4-benzoquinone (23)

Synthesized using the same general procedure described for the synthesis of **1**, commencing with 1,4-benzoquinone and 4-hydroxybenzylamine to afford the title compound as a dark pink solid. Yield 0.170 g (54%); mp 242 °C.

1H NMR (DMSO- d_6) δ 4.22 (4H, d, J = 6.6 Hz), 5.18 (2H, s), 6.69 (4H, d, J = 8.7 Hz), 7.08 (4H, d, J = 8.7 Hz), 8.11 (2H, t, J = 6.6 Hz, NH), 9.33 (2H, br s, OH).

^{13}C NMR (DMSO- d_6) δ 45.0 (2C), 93.2 (2C), 115.4 (4C), 127.6 (2C), 128.8 (4C), 151.1 (2C), 156.7 (2C), 177.9 (2C).

MS (ESI+) m/z : 351 (M+H), HRMS (ESI+) m/z calculated for $C_{20}H_{18}N_2O_4$ (M+H) 351.1345; found 351.1339.

4.3.23. 2,5-Bis(4-chlorobenzylamino)-1,4-benzoquinone (24)

Synthesized using the same general procedure described for the synthesis of **1**, commencing with 1,4-benzoquinone and 4-chlorobenzylamine to afford the title compound as an orange-brown solid. Yield 0.277 g (58%); mp 222–224 °C.

1H NMR (DMSO- d_6) δ 4.34 (4H, d, J = 6.6 Hz), 5.16 (2H, s), 7.30 (4H, d, J = 8.7 Hz), 7.38 (4H, d, J = 8.7 Hz), 8.29 (2H, t, J = 6.6 Hz, NH).

^{13}C NMR (DMSO- d_6) δ 44.6 (2C), 93.6 (2C), 128.7 (4C), 129.3 (4C), 131.9 (2C), 136.7 (2C), 151.0 (2C), 178.1 (2C).

MS (ESI+) m/z : 387 (M+H), HRMS (ESI+) m/z calculated for $C_{20}H_{16}Cl_2N_2O_2$ (M+H) 387.0667; found 387.0662.

4.3.24. 2,5-Bis(phenethylamino)-1,4-benzoquinone (25)

Synthesized using the same general procedure described for the synthesis of **1**, commencing with 1,4-benzoquinone and phenethylamine to afford the title compound as a red-brown solid. Yield 0.375 g (61%); mp 218–220 °C (Lit. 222 °C) [46].

1H NMR (DMSO- d_6) δ 2.85 (4H, m), 3.37 (4H, m), 5.27 (2H, s), 7.23 (10H, m), 7.64 (2H, t, J = 6.3 Hz, NH).

^{13}C NMR (DMSO- d_6) δ 33.6 (2C), 43.3 (2C), 92.4 (2C), 126.5 (2C), 128.5 (4C), 128.9 (4C), 138.9 (2C), 151.1 (2C), 177.5 (2C).

MS (ESI+) m/z : 347 (M+H), HRMS (ESI+) m/z calculated for $C_{22}H_{22}N_2O_2$ (M+H) 347.1760; found 347.1754.

4.3.25. 2,5-Bis(ethylamino)-1,4-benzoquinone (**26**)

Synthesized using the same general procedure described for the synthesis of **1**, commencing with 1,4-benzoquinone and ethylamine to afford the title compound as a pink-brown solid. Yield 0.071 g (39%); mp 209–210 °C (Lit. 218 °C; 210 °C) [44].

1H NMR (DMSO- d_6) δ 1.11 (6H, t, J = 7.2 Hz), 3.15 (4H, m), 5.21 (2H, s), 7.65 (2H, t, J = 6.3 Hz, NH).

^{13}C NMR (DMSO- d_6) δ 13.3 (2C), 36.8 (2C), 92.0 (2C), 151.3 (2C), 177.5 (2C).

MS (ESI+) m/z : 195 (M+H), HRMS (ESI+) m/z calculated for $C_{10}H_{14}N_2O_2$ (M+H) 195.1134; found 195.1128.

4.3.26. 2,5-Bis(propylamino)-1,4-benzoquinone (**27**)

Synthesized using the same general procedure described for the synthesis of **1**, commencing with 1,4-benzoquinone and propylamine to afford the title compound as a pink solid. Yield 0.075 g (37%); mp 142–143 °C.

1H NMR (DMSO- d_6) δ 0.85 (6H, t, J = 7.5 Hz), 1.55 (4H, m), 3.08 (4H, m), 5.23 (2H, s), 7.69 (2H, t, J = 6.3 Hz, NH).

^{13}C NMR (DMSO- d_6) δ 11.4 (2C₃), 21.0 (2C), 43.6 (2C), 92.1 (2C), 151.6 (2C), 177.4 (2C).

MS (ESI+) m/z : 223 (M+H), HRMS (ESI+) m/z calculated for $C_{12}H_{18}N_2O_2$ (M+H) 223.1447; found 223.1441.

4.3.27. 2,5-Bis(butylamino)-1,4-benzoquinone (**28**)

Synthesized using the same general procedure described for the synthesis of **1**, commencing with 1,4-benzoquinone and butylamine to afford the title compound as an orange-pink solid. Yield 0.070 g (30%); mp 149–150 °C (Lit. 160 °C; 154 °C) [42].

1H NMR (DMSO- d_6) δ 0.87 (6H, t, J = 7.2 Hz), 1.29 (4H, m), 1.50 (4H, m), 3.11 (4H, m), 5.22 (2H, s), 7.69 (2H, t, J = 6.3 Hz, NH).

^{13}C NMR (DMSO- d_6) δ 13.8 (2C), 19.8 (2C), 29.7 (2C), 41.7 (2C), 92.0 (2C), 151.5 (2C), 177.4 (2C).

MS (ESI+) m/z : 251 (M+H), HRMS (ESI+) m/z calculated for $C_{14}H_{22}N_2O_2$ (M+H) 251.1760; found 251.1754.

4.3.28. 2,5-Bis(pentylamino)-1,4-benzoquinone (**29**)

Synthesized using the same general procedure described for the synthesis of **1**, commencing with 1,4-benzoquinone and pentylamine to afford the title compound as a pink-red solid. Yield 0.171 g (66%); mp 133–134 °C (Lit. 134.6–137.1 °C) [36].

1H NMR (DMSO- d_6) δ 0.85 (6H, t, J = 6.9 Hz), 1.26 (8H, m), 1.52 (4H, m), 3.11 (4H, m), 5.21 (2H, s), 7.69 (1H, t, J = 6.3 Hz, NH).

^{13}C NMR (DMSO- d_6) δ 14.0 (2C), 21.9 (2C), 27.3 (2C), 28.8 (2C), 41.9 (2C), 92.0 (2C), 151.5 (2C), 177.4 (2C).

MS (ESI+) m/z : 279 (M+H), HRMS (ESI+) m/z calculated for $C_{16}H_{26}N_2O_2$ (M+H) 279.2073; found 279.2067.

4.3.29. 2,5-Bis(hexylamino)-1,4-benzoquinone (**30**)

Synthesized using the same general procedure described for the synthesis of **1**, commencing with 1,4-benzoquinone and *n*-hexylamine to afford the title compound as a bright orange-pink solid. Yield 0.162 g (56%); mp 130–132 °C (Lit. 114–116 °C) [47].

1H NMR (DMSO- d_6) δ 0.85 (6H, t, J = 6.9 Hz), 1.25 (12H, m), 1.51 (4H, m), 3.11 (4H, m), 5.21 (2H, s), 7.69 (2H, t, J = 6.0 Hz, NH).

^{13}C NMR (DMSO- d_6) δ 14.0 (2C), 22.2 (2C), 26.2 (2C), 27.6 (2C), 31.0 (2C), 42.0 (2C), 92.0 (2C), 151.5 (2C), 177.4 (2C).

MS (ESI+) m/z : 307 (M+H), HRMS (ESI+) m/z calculated for $C_{18}H_{30}N_2O_2$ (M+H) 307.2386; found 307.2380.

4.3.30. 2,5-Bis(isopentylamino)-1,4-benzoquinone (**31**)

Synthesized using the same general procedure described for the synthesis of **1**, commencing with 1,4-benzoquinone and iso-pentylamine to afford the title compound as an orange-pink solid. Yield 0.117 g (49%); mp 164–165 °C (Lit. 167.3–169.7 °C) [36].

1H NMR (DMSO- d_6) δ 0.88 (12H, d, J = 6.6 Hz), 1.42 (4H, m), 1.56 (2H, m), 3.13 (4H, m), 5.20 (2H, s), 7.67 (2H, t, J = 6.3 Hz, NH).

^{13}C NMR (DMSO- d_6) δ 22.4 (4C), 25.6 (2C), 36.3 (2C), 40.3 (2C), 92.0 (2C), 151.4 (2C), 177.4 (2C).

MS (ESI+) m/z : 279 (M+H), HRMS (ESI+) m/z calculated for $C_{16}H_{26}N_2O_2$ (M+H) 279.2073; found 279.2067.

4.3.31. 2,5-Bis(allylamino)-1,4-benzoquinone (**32**)

Synthesized using the same general procedure described for the synthesis of **1**, commencing with 1,4-benzoquinone and allylamine to afford the title compound as a pink-red solid. Yield 0.172 g (79%); mp 192–193 °C (Lit. 170 °C; 192–193 °C) [48].

1H NMR (DMSO- d_6) δ 3.79 (4H, m), 5.11 (2H, m), 5.16 (2H, dd, J = 1.8, 6.6 Hz), 5.19 (2H, s), 5.77 (2H, m), 7.84 (2H, t, J = 6.3 Hz, NH).

^{13}C NMR (DMSO- d_6) δ 44.3 (2C), 93.1 (2C), 116.7 (2C), 133.1 (2C), 151.2 (2C), 177.8 (2C) ppm.

MS (ESI+) m/z : 219 (M+H), HRMS (ESI+) m/z calculated for $C_{12}H_{14}N_2O_2$ (M+H) 219.1134; found 219.1128.

4.3.32. 2,5-Bis(3-bromopropylamino)-1,4-benzoquinone (**33**)

Synthesized using the same general procedure described for the synthesis of **1**, commencing with 1,4-benzoquinone and 3-bromopropylamine hydrobromide. A stoichiometric quantity of triethylamine was added to the reaction mixture to neutralize the liberated HBr. The title compound was obtained as a brown solid. Yield 0.230 g (67%); mp 180–181 °C.

1H NMR (DMSO- d_6) δ 2.06 (4H, m), 3.24 (4H, m), 3.53 (4H, t, J = 6.6 Hz), 5.29 (2H, s), 7.78 (2H, t, J = 6.3 Hz, NH).

^{13}C NMR (DMSO- d_6) δ 30.9 (2C), 32.3 (2C), 40.6 (2C), 92.5 (2C), 151.4 (2C), 177.7 (2C).

MS (ESI+) m/z : 379 (M+H), HRMS (ESI+) m/z calculated for $C_{12}H_{16}Br_2N_2O_2$ (M+H) 378.9657; found 378.9651.

4.3.33. 2,5-Bis(2-hydroxyethylamino)-1,4-benzoquinone (**34**)

Synthesized using the same general procedure described for the synthesis of **1**, commencing with 1,4-benzoquinone and ethanolamine to afford the title compound as a red-brown solid. Yield 0.224 g (60%); mp 244–246 °C (Lit. > 350 °C) [35].

1H NMR (DMSO- d_6) δ 3.18 (4H, m), 3.54 (4H, q, J = 5.4 Hz), 4.88 (2H, t, J = 5.4 Hz, OH), 5.28 (2H, s), 7.51 (2H, t, J = 5.1 Hz, NH).

^{13}C NMR (DMSO- d_6) δ 44.8 (2C), 58.6 (2C), 92.4 (2C), 151.7 (2C), 177.6 (2C).

MS (ESI+) m/z : 227 (M+H), HRMS (ESI+) m/z calculated for $C_{10}H_{14}N_2O_4$ (M+H) 227.1032; found 227.1026.

4.3.34. 2,5-Bis(3-hydroxypropylamino)-1,4-benzoquinone (**35**)

Synthesized using the same general procedure described for the synthesis of **1**, commencing with 1,4-benzoquinone and 3-amino-1-propanol to afford the title compound as a red-brown solid. Yield 0.227 g (55%); mp 160–162 °C.

1H NMR (DMSO- d_6) δ 1.67 (4H, m), 3.18 (4H, m), 3.44 (4H, m), 4.62 (2H, t, J = 4.8 Hz, OH), 5.23 (2H, s), 7.76 (2H, t, J = 6.0 Hz, NH).

^{13}C NMR (DMSO- d_6) δ 30.7 (2C), 39.7 (2C), 58.8 (2C), 92.1 (2C), 151.6 (2C), 177.4 (2C).

MS (ESI+) m/z : 255 (M+H), HRMS (ESI+) m/z calculated for $C_{12}H_{18}N_2O_4$ (M+H) 255.1345; found 255.1339.

4.3.35. 2,5-Bis(4-hydroxybutylamino)-1,4-benzoquinone (**36**)

Synthesized using the same general procedure described for the synthesis of **1**, commencing with 1,4-benzoquinone and 4-amino-

1-butanol to afford the title compound as an orange-brown solid. Yield 0.139 g (54%); mp 122–124 °C.

^1H NMR (DMSO- d_6) δ 1.41 (4H, m), 1.55 (4H, m), 3.13 (4H, m), 3.38 (4H, m), 4.42 (2H, t, J = 5.1 Hz, OH), 5.23 (2H, s), 7.74 (2H, t, J = 6.0 Hz, NH).

^{13}C NMR (DMSO- d_6) δ 24.5 (2C), 30.0 (2C), 41.9 (2C), 60.5 (2C), 92.1 (2C), 151.6 (2C), 177.4 (2C).

MS (ESI+) m/z : 283 (M+H), HRMS (ESI+) m/z calculated for $\text{C}_{14}\text{H}_{22}\text{N}_2\text{O}_4$ (M+H) 283.1658; found 283.1652.

4.3.36. 2,5-Bis(2-methoxyethylamino)-1,4-benzoquinone (37)

To a stirred solution of 1,4-benzoquinone (0.542 g, 5.01 mmol) in methanol (10 mL) was added 2-methoxyethylamine (3.33 mmol). The resulting dark red solution was stirred at 25 °C for 18 h, during which time a red-brown solid began to precipitate. The reaction mixture was kept at 4 °C for 24 h. The precipitate was collected by filtration, washed sequentially with methanol and ether, and dried under vacuum to afford the title compound as purple flakes. Yield 0.103 g (44%); mp 125–126 °C.

^1H NMR (DMSO- d_6) δ 3.24 (6H, s), 3.29 (4H, q, J = 5.7 Hz), 3.49 (4H, t, J = 5.7 Hz), 5.29 (2H, s), 7.52 (2H, t, J = 5.7 Hz, NH).

^{13}C NMR (DMSO- d_6) δ 41.7 (2C), 58.2 (2C), 69.3 (2C), 92.4 (2C), 151.4 (2C), 177.6 (2C).

MS (ESI+) m/z : 255 (M+H), HRMS (ESI+) m/z calculated for $\text{C}_{12}\text{H}_{18}\text{N}_2\text{O}_4$ (M+H) 255.1345; found 255.1339.

4.3.37. 2,5-Bis(3-methoxypropylamino)-1,4-benzoquinone (38)

Synthesized using the same general procedure described for the synthesis of **1**, commencing with 1,4-benzoquinone and 3-methoxypropylamine to afford the title compound as a light pink solid. Yield 0.124 g (47%); mp 100–102 °C.

^1H NMR (DMSO- d_6) δ 1.76 (4H, m), 3.17 (4H, m), 3.22 (6H, s), 3.34 (4H, t, J = 6.0 Hz), 5.20 (2H, s), 7.70 (2H, t, J = 6.0 Hz, NH).

^{13}C NMR (DMSO- d_6) δ 27.8 (2C), 39.6 (2C), 58.1 (2C), 69.8 (2C), 92.1 (2C), 151.5 (2C), 177.5 (2C).

MS (ESI+) m/z : 283 (M+H), HRMS (ESI+) m/z calculated for $\text{C}_{14}\text{H}_{22}\text{N}_2\text{O}_4$ (M+H) 283.1658; found 283.1652.

4.3.38. 2,5-Bis(2-(methylthio)ethylamino)-1,4-benzoquinone (39)

Synthesized using the same general procedure described for the synthesis of **1**, commencing with 1,4-benzoquinone and 2-(methylthio)ethylamine to afford the title compound as a brick-red solid. Yield 0.321 g (70%); mp 157–158 °C.

^1H NMR (DMSO- d_6) δ 2.08 (6H, s), 2.68 (4H, m), 3.34 (4H, m), 5.30 (2H, s), 7.68 (2H, t, J = 6.0 Hz, NH).

^{13}C NMR (DMSO- d_6) δ 14.6 (2C), 31.3 (2C), 41.1 (2C), 92.5 (2C), 151.1 (2C), 177.7 (2C).

MS (ESI+) m/z : 287 (M+H), HRMS (ESI+) m/z calculated for $\text{C}_{12}\text{H}_{18}\text{N}_2\text{O}_2\text{S}_2$ (M+H) 287.0888; found 287.0882.

4.3.39. 2,5-Bis(2-(dimethylamino)ethylamino)-1,4-benzoquinone (40)

Synthesized using the same general procedure described for the synthesis of **37**, commencing with 1,4-benzoquinone and *N,N*-dimethylethylenediamine to afford the title compound as a bright pink solid. Yield 0.273 g (61%); mp 146–148 °C (Lit. 155–159 °C) [49].

^1H NMR (DMSO- d_6) δ 2.16 (12H, s), 2.45 (4H, t, J = 6.3 Hz), 3.19 (4H, m), 5.25 (2H, s), 7.39 (2H, t, J = 5.7 Hz, NH).

^{13}C NMR (DMSO- d_6) δ 39.6 (2C), 45.1 (4C), 56.3 (2C), 92.3 (2C), 151.2 (2C), 177.4 (2C).

MS (ESI+) m/z : 281 (M+H), HRMS (ESI+) m/z calculated for $\text{C}_{14}\text{H}_{24}\text{N}_4\text{O}_2$ (M+H) 281.1978; found 281.1972.

4.3.40. 2,5-Bis(2-chloroethylamino)-1,4-benzoquinone (41)

Synthesized using the same general procedure described for the synthesis of **1**, commencing with 1,4-benzoquinone and 2-chloroethylamine hydrochloride. A stoichiometric quantity of triethylamine was added to the reaction mixture to neutralize the liberated HCl. The title compound was obtained as a brown solid. Yield 0.187 g (75%); mp 190–191 °C.

^1H NMR (DMSO- d_6) δ 3.50 (4H, m), 3.78 (4H, t, J = 6.0 Hz), 5.37 (2H, s), 7.70 (2H, t, J = 6.3 Hz, NH).

^{13}C NMR (DMSO- d_6) δ 42.2 (2C), 43.7 (2C), 93.1 (2C), 151.0 (2C), 178.0 (2C).

MS (ESI+) m/z : 263 (M+H), HRMS (ESI+) m/z calculated for $\text{C}_{10}\text{H}_{12}\text{Cl}_2\text{N}_2\text{O}_2$ (M+H) 263.0354; found 263.0349.

4.3.41. 2,5-Bis(2-bromoethylamino)-1,4-benzoquinone (42)

Synthesized using the same general procedure described for the synthesis of **1**, commencing with 1,4-benzoquinone and 2-bromoethylamine hydrobromide. A stoichiometric quantity of triethylamine was added to the reaction mixture to neutralize the liberated HBr. The title compound was obtained as a brown solid. Yield 0.202 g (67%); mp 160–161 °C.

^1H NMR (DMSO- d_6) δ 3.61 (8H, m), 5.37 (2H, s), 7.72 (2H, t, J = 6.0 Hz, NH).

^{13}C NMR (DMSO- d_6) δ 30.8 (2C), 43.6 (2C), 93.1 (2C), 150.8 (2C), 178.1 (2C).

MS (ESI+) m/z : 351 (M+H), HRMS (ESI+) m/z calculated for $\text{C}_{10}\text{H}_{12}\text{Br}_2\text{N}_2\text{O}_2$ (M+H) 350.9344; found 350.9338.

4.3.42. 2,5-Bis(3-chloropropylamino)-1,4-benzoquinone (43)

Synthesized using the same general procedure described for the synthesis of **1**, commencing with 1,4-benzoquinone and 3-chloropropylamine hydrochloride. A stoichiometric quantity of triethylamine was added to the reaction mixture to neutralize the liberated HCl. The title compound was obtained as a light brown solid. Yield 0.220 g (61%); mp 178–180 °C.

^1H NMR (DMSO- d_6) δ 1.98 (4H, m), 3.25 (4H, m), 3.65 (4H, t, J = 6.6 Hz), 5.28 (2H, s), 7.78 (2H, t, J = 6.3 Hz, NH).

^{13}C NMR (DMSO- d_6) δ 30.7 (2C), 39.5 (2C), 43.1 (2C), 92.5 (2C), 151.5 (2C), 177.8 (2C).

MS (ESI+) m/z : 291 (M+H), HRMS (ESI+) m/z calculated for $\text{C}_{12}\text{H}_{16}\text{Cl}_2\text{N}_2\text{O}_2$ (M+H) 291.0667; found 291.0662.

4.3.43. 2,5-Bis(4-hydroxyanilino)-1,4-benzoquinone (45)

Synthesized using the same general procedure described for the synthesis of **1**, commencing with 1,4-benzoquinone and 4-aminophenol to afford the title compound as a dark brown solid. Yield 0.193 g (39%); mp > 250 °C.

^1H NMR (DMSO- d_6) δ 5.54 (2H, s), 6.80 (4H, d, J = 8.7 Hz), 7.14 (4H, d, J = 8.7 Hz), 9.16 (2H, br s, NH), 9.58 (2H, br s, OH).

^{13}C NMR (DMSO- d_6) δ 94.2 (2C), 115.9 (4C), 125.7 (4C), 129.0 (2C), 148.6 (2C), 155.6 (2C), 179.2 (2C).

MS (ESI+) m/z : 323 (M+H), HRMS (ESI+) m/z calculated for $\text{C}_{18}\text{H}_{14}\text{N}_2\text{O}_4$ (M+H) 323.1032; found 323.1026.

4.3.44. 2,5-Bis(phenylamino)-1,4-benzoquinone (46)

Synthesized using the same general procedure described for the synthesis of **1**, commencing with 1,4-benzoquinone and aniline hydrobromide to afford the title compound as a dark purple solid. Yield 0.091 g (54%); mp > 250 °C (Lit. > 350 °C; 357–360 °C; 345 °C) [42].

^1H NMR (DMSO- d_6) (50 °C) δ 5.78 (2H, s), 7.22 (2H, m), 7.40 (8H, m), 9.27 (2H, br s, NH).

^{13}C NMR (DMSO- d_6) (50 °C) δ 95.7 (2C), 123.3 (2C), 125.3 (2C), 129.1 (2C), 137.8 (2C), 147.2 (2C), 179.6 (2C).

MS (ESI+) m/z : 291 (M+H), HRMS (ESI+) m/z calculated for $C_{18}H_{14}N_2O_2$ (M+H) 291.1134; found 291.1128.

4.3.45. 2,5-Bis(2-carboxyanilino)-1,4-benzoquinone (47)

Synthesized using the same general procedure described for the synthesis of **1**, commencing with 1,4-benzoquinone and anthranilic acid to afford the title compound as a dark red-brown solid. Yield 0.290 g (63%) mp > 250 °C (Lit. 322–324 °C; 335 °C; 315 °C) [50].

1H NMR (DMSO- d_6) δ 6.24 (2H, s), 7.26 (2H, m), 7.68 (4H, m), 8.02 (2H, m, H), 10.73 (2H, br s, NH).

^{13}C NMR (DMSO- d_6) δ 98.4 (2C), 120.8 (2C), 121.4 (2C), 124.1 (2C), 132.1 (2C), 134.1 (2C), 139.5 (2C), 144.5 (2C), 168.4 (2C), 180.8 (2C).

MS (ESI-) m/z : 377 (M-H), HRMS (ESI-) m/z calculated for $C_{20}H_{14}N_2O_6$ (M-H) 377.0774; found 377.0779.

4.3.46. 2,5-Bis(3-carboxyanilino)-1,4-benzoquinone (48)

Synthesized using the same general procedure described for the synthesis of **1**, commencing with 1,4-benzoquinone and 3-aminobenzoic acid to afford the title compound as an olive-green solid. Yield 0.139 g (60%). mp > 250 °C.

1H NMR (DMSO- d_6) δ 5.81 (2H, s), 7.55 (2H, t, J = 7.8 Hz), 7.62 (2H, m), 7.78 (2H, m), 7.90 (2H, t, J = 1.8 Hz), 9.42 (2H, br s, NH), 13.12 (2H, br s, COOH).

^{13}C NMR (DMSO- d_6) δ 96.0 (2C), 124.3 (2C), 126.4 (2C), 128.2 (2C), 129.8 (2C), 132.1 (2C), 138.3 (2C), 147.2 (2C), 166.9 (2C), 180.1 (2C).

MS (ESI-) m/z : 377 (M-H), HRMS (ESI-) m/z calculated for $C_{20}H_{14}N_2O_6$ (M-H) 377.0774; found 377.0779.

4.3.47. 2,5-Bis(4-carboxyanilino)-1,4-benzoquinone (49)

Synthesized using the same general procedure described for the synthesis of **1**, commencing with 1,4-benzoquinone and 4-aminobenzoic acid to afford the title compound as a dark brown solid. Yield 0.160 g (68%); mp > 250 °C (Lit. > 260 °C) [51].

1H NMR (DMSO- d_6) δ 6.06 (2H, s), 7.52 (4H, d, J = 8.7 Hz), 7.96 (4H, d, J = 8.7 Hz), 9.44 (2H, br s, NH).

^{13}C NMR (DMSO- d_6) δ 97.8 (2C), 123.0 (4C), 127.2 (2C), 131.0 (4C), 142.4 (2C), 146.1 (2C), 167.2 (2C), 180.8 (2C).

MS (ESI-) m/z : 377 (M-H), HRMS (ESI-) m/z calculated for $C_{20}H_{14}N_2O_6$ (M-H) 377.0774; found 377.0779.

4.3.48. 2,5-Bis(3-hydroxyanilino)-1,4-benzoquinone (50)

Synthesized using the same general procedure described for the synthesis of **1**, commencing with 1,4-benzoquinone and 3-aminophenol to afford the title compound as a dark brown solid. Yield 0.071 g (37%); mp > 250 °C.

1H NMR (DMSO- d_6) δ 5.81 (2H, s), 6.61 (2H, dd, J = 2.1, 7.8 Hz), 6.79 (4H, m), 7.20 (2H, dd, J = 7.8, 8.1 Hz), 9.18 (2H, br s, NH), 9.63 (2H, br s, OH).

^{13}C NMR (DMSO- d_6) δ 95.8 (2C), 110.5 (2C), 112.9 (2C), 114.4 (2C), 130.2 (2C), 138.9 (2C), 147.3 (2C), 158.2 (2C), 179.9 (2C).

MS (ESI+) m/z : 323 (M+H), HRMS (ESI+) m/z calculated for $C_{18}H_{14}N_2O_4$ (M+H) 323.1032; found 323.1026.

4.3.49. 2,5-Bis(2-methylanilino)-1,4-benzoquinone (51)

Synthesized using the same general procedure described for the synthesis of **1**, commencing with 1,4-benzoquinone and *o*-toluidine to afford the title compound as dark purple flakes. Yield 0.096 g (49%); mp > 250 °C (253–254 °C; 250–252 °C) [52].

1H NMR (DMSO- d_6) δ 2.17 (6H, s), 5.01 (2H, s), 7.21 (2H, m), 7.27 (4H, m), 7.34 (2H, m), 9.11 (2H, br s, NH).

^{13}C NMR (DMSO- d_6) δ 17.5 (2C), 94.5 (2C), 126.6 (2C), 127.0 (2C), 127.4 (2C), 131.2 (2C), 134.4 (2C), 136.2 (2C), 149.8 (2C), 179.0 (2C).

MS (ESI+) m/z : 319 (M+H), HRMS (ESI+) m/z calculated for $C_{20}H_{18}N_2O_2$ (M+H) 319.1447; found 319.1441.

4.3.50. 2,5-Bis(2-methoxyanilino)-1,4-benzoquinone (52)

Synthesized using the same general procedure described for the synthesis of **37**, commencing with 1,4-benzoquinone and *o*-anisidine to afford the title compound as a brown solid. Yield 0.286 g (49%); mp 240–241 °C (Lit. 250 °C) [52].

1H NMR (DMSO- d_6) δ 3.84 (6H, s), 5.56 (2H, s), 7.02 (2H, td, J = 0.9, 7.5 Hz), 7.15 (2H, dd, J = 0.9, 7.8 Hz), 7.26 (2H, td, J = 1.2, 7.8 Hz), 7.36 (2H, dd, J = 1.2, 7.8 Hz), 8.84 (2H, br s, NH).

^{13}C NMR (100 MHz) (DMSO- d_6) δ 56.0 (2C), 95.6 (2C), 112.3 (2C), 121.0 (2C), 123.8 (2C), 126.0 (2C), 127.2 (2C), 146.9 (2C), 152.3 (2C), 179.4 (2C).

MS (ESI+) m/z : 351 (M+H), HRMS (ESI+) m/z calculated for $C_{20}H_{18}N_2O_4$ (M+H) 351.1345; found 351.1339.

4.3.51. 2,5-Bis(3-methoxyanilino)-1,4-benzoquinone (53)

Synthesized using the same general procedure described for the synthesis of **1**, commencing with 1,4-benzoquinone and *m*-anisidine to afford the title compound as a dark brown solid. Yield 0.096 g (51%); mp > 250 °C.

1H NMR (DMSO- d_6) δ 3.76 (6H, s), 5.82 (2H, s), 6.80 (2H, m), 6.94 (2H, m), 6.96 (2H, m), 7.33 (2H, t, J = 8.4 Hz), 9.24 (2H, br s, NH).

^{13}C NMR (100 MHz) (DMSO- d_6) δ 55.4 (2C), 96.0 (2C), 109.7 (2C), 111.3 (2C), 115.7 (2C), 130.2 (2C), 139.1 (2C), 147.2 (2C), 160.0 (2C), 180.0 (2C).

MS (ESI+) m/z : 351 (M+H), HRMS (ESI+) m/z calculated for $C_{20}H_{18}N_2O_4$ (M+H) 351.1345; found 351.1339.

4.3.52. 2,5-Bis(4-methoxyanilino)-1,4-benzoquinone (54)

Synthesized using the same general procedure described for the synthesis of **1**, commencing with 1,4-benzoquinone and *p*-anisidine. The title compound was obtained as a dark brown solid. Yield 0.167 g (53%); mp > 250 °C.

1H NMR (DMSO- d_6) δ 3.76 (6H, s), 5.60 (2H, s), 6.99 (4H, d, J = 9.0 Hz), 7.27 (4H, d, J = 9.0 Hz), 9.23 (2H, br s, NH).

^{13}C NMR (DMSO- d_6) δ 55.6 (2C), 95.8 (2C), 114.9 (4C), 125.8 (4C), 130.7 (2C), 147.1 (2C), 157.2 (2C), 179.9 (2C).

MS (ESI+) m/z : 351 (M+H), HRMS (ESI+) m/z calculated for $C_{20}H_{18}N_2O_4$ (M+H) 351.1345; found 351.1339.

4.3.53. 2,5-Bis(2-bromoanilino)-1,4-benzoquinone (55)

Synthesized using the same general procedure described for the synthesis of **1**, commencing with 1,4-benzoquinone and 2-bromoaniline to afford the title compound as a brown solid. Yield 0.103 g (37%); mp 225–226 °C.

1H NMR (DMSO- d_6) δ 5.18 (2H, s), 7.29 (2H, m), 7.45 (2H, m), 7.49 (2H, m), 7.78 (2H, m), 9.15 (2H, br s, NH);

^{13}C NMR (100 MHz) (DMSO- d_6) δ 95.9 (2C), 120.3 (2C), 127.9 (2C), 129.0 (2C), 129.1 (2C), 133.6 (2C), 136.2 (2C), 148.3 (2C), 179.3 (2C).

MS (ESI+) m/z : 447 (M+H), HRMS (ESI+) m/z calculated for $C_{18}H_{12}Br_2N_2O$ (M+H) 446.9344; found 446.9339.

4.3.54. 2,5-Bis(2-(hydroxymethyl)anilino)-1,4-benzoquinone (56)

Synthesized using the same general procedure described for the synthesis of **1**, commencing with 1,4-benzoquinone and 2-aminobenzyl alcohol to afford the title compound as a yellow-brown solid. Yield 0.090 g (45%); mp 206–207 °C.

1H NMR (DMSO- d_6) δ 4.47 (4H, s), 5.47 (2H, br s, OH), 5.50 (2H, s), 7.26 (2H, m), 7.37 (4H, m), 7.46 (2H, d, J = 7.5 Hz), 9.33 (2H, br s, NH).

^{13}C NMR (100 MHz) (DMSO- d_6) δ 60.7 (2C), 95.2 (2C), 124.3 (2C), 126.3 (2C), 128.2 (2C), 128.8 (2C), 136.0 (2C), 136.4 (2C), 148.1 (2C), 179.5 (2C).

MS (ESI+) m/z : 351 (M+H), HRMS (ESI+) m/z calculated for $C_{20}H_{18}N_2O_4$ (M+H) 351.1345; found 351.1339.

4.3.55. 2,5-Bis(3-(hydroxymethyl)phenylamino)-1,4-benzoquinone (57)

Synthesized using the same general procedure described for the synthesis of **37**, commencing with 1,4-benzoquinone and 3-aminobenzylalcohol to afford the title compound as a brown solid. Yield 0.294 g (51%); mp 243–244 °C.

¹H NMR (DMSO-*d*₆) δ 4.51 (4H, d, *J* = 5.7 Hz), 5.26 (2H, t, *J* = 5.7 Hz, OH), 5.80 (2H, s), 7.16 (2H, m), 7.22 (2H, m), 7.32 (2H, m), 7.37 (2H, t, *J* = 7.8 Hz), 9.27 (2H, br s, NH).

¹³C NMR (DMSO-*d*₆) δ 62.7 (2C), 95.5 (2C), 121.5 (2C), 122.3 (2C), 123.8 (2C), 129.2 (2C), 137.8 (2C), 144.1 (2C), 147.5 (2C), 179.9 (2C).

MS (ESI+) *m/z*: 351 (M+H), HRMS (ESI+) *m/z* calculated for C₂₀H₁₈N₂O₄ (M+H) 351.1345; found 351.1339.

4.3.56. 2,5-Bis(4-(hydroxymethyl)phenylamino)-1,4-benzoquinone (58)

Synthesized using the same general procedure described for the synthesis of **37**, commencing with 1,4-benzoquinone and 4-aminobenzylalcohol to afford the title compound as a brown solid. Yield 0.197 g (47%); mp > 250 °C.

¹H NMR (DMSO-*d*₆) δ 4.49 (4H, d, *J* = 5.7 Hz), 5.19 (2H, t, *J* = 5.7 Hz, OH), 5.75 (2H, s), 7.31 (4H, d, *J* = 8.7 Hz), 7.36 (4H, d, *J* = 8.7 Hz), 9.28 (2H, br s, NH).

¹³C NMR (DMSO-*d*₆) δ 62.7 (2C), 95.3 (2C), 123.6 (4C), 127.5 (4C), 136.4 (2C), 140.2 (2C), 147.6 (2C), 179.8 (2C).

MS (ESI+) *m/z*: 351 (M+H), HRMS (ESI+) *m/z* calculated for C₂₀H₁₈N₂O₄ (M+H) 351.1345; found 351.1339.

Author statement

The authors declare the following competing financial interest(s): We have entered into a commercial agreement with Abcam Biochemicals (Cambridge, UK) for the supply of our dynamin inhibitors. This includes some of the compounds listed in this paper.

[#]Dynole™, Rhododyn™, MiTMAB™, Bis-T™, Dyngo™, and Imidyn™ are trademarks of Children's Medical Research Institute and Newcastle Innovation Ltd. Most of the lead dynamin inhibitors described in this paper are available from Abcam Biochemicals (Cambridge, UK).

Acknowledgements

This work was supported by grants from the National Health and Medical Research Council (Australia) (Grant 571076 and 1011457), The Australia Research Council, The Australian Cancer Research Foundation, The Ramaciotti Foundation, The Children's Medical Research Institute, and Newcastle Innovation Ltd.

Abbreviations

CME	Clathrin-Mediated Endocytosis
SVE	Synaptic Vesicle Endocytosis
MiTMAB	myristoyl trimethyl ammonium bromide
OcTMAB	Octyl trimethyl ammonium bromide
Bis-T	Bis-tyrphostin
RTIL	Room Temperature Ionic Liquid
PSA	Polar Surface Area
U2OS	Human Bone Osteosarcoma Epithelial Cells
DynI	Dynamin I
DynII	Dynamin II
FL-Dyn I	full length dynamin I;
FL-Dyn II	full length dynamin II.

Appendix A. Supplementary data

Supplementary data related to this article can be found at <http://dx.doi.org/10.1016/j.ejmech.2014.06.070>.

References

- [1] S.M. Ferguson, P. De Camilli, Dynamin, a membrane-remodelling GTPase, *Nat. Rev. Mol. Cell Biol.* 13 (2012) 75–88.
- [2] J.S. Chappie, S. Acharya, M. Leonard, S.L. Schmid, F. Dyda, G domain dimerization controls dynamin's assembly-stimulated GTPase activity, *Nature* 465 (2010) 435–440.
- [3] Joshua S. Chappie, Jason A. Mears, S. Fang, M. Leonard, Sandra L. Schmid, Ronald A. Milligan, Jenny E. Hinshaw, F. Dyda, A pseudoatomic model of the dynamin polymer identifies a hydrolysis-dependent powerstroke, *Cell* 147 (2011) 209–222.
- [4] B. Marks, M.H.B. Stowell, Y. Vallis, I.G. Mills, A. Gibson, C.R. Hopkins, H.T. McMahon, GTPase activity of dynamin and resulting conformation change are essential for endocytosis, *Nature* 410 (2001) 231–235.
- [5] G.J.K. Praefcke, H.T. McMahon, The dynamin superfamily: universal membrane tubulation and fission molecules, *Nat. Rev. Mol. Cell Biol.* 5 (2004) 133–147.
- [6] K.M. Ferguson, M.A. Lemmon, J. Schlessinger, P.B. Sigler, Crystal structure at 2.2 Å resolution of the pleckstrin homology domain from human dynamin, *Cell* 79 (1994) 199–209.
- [7] T.F. Reubold, S. Eschenburg, A. Becker, M. Leonard, S.L. Schmid, R.B. Vallee, F.J. Kull, D.J. Manstein, Crystal structure of the GTPase domain of rat dynamin 1, *Proc. Natl. Acad. Sci. U. S. A.* 102 (2005) 13093–13098.
- [8] H.H. Niemann, M.L.W. Knetsch, A. Scherer, D.J. Manstein, F.J. Kull, Crystal structure of a dynamin GTPase domain in both nucleotide-free and GDP-bound forms, *EMBO J.* 20 (2001) 5813–5821.
- [9] S. Gao, A. von der Malsburg, S. Paeschke, J. Behlke, O. Haller, G. Kochs, O. Daumke, Structural basis of oligomerization in the stalk region of dynamin-like MxA, *Nature* 465 (2010) 502–506.
- [10] H.T. McMahon, E. Boucrot, Molecular mechanism and physiological functions of clathrin-mediated endocytosis, *Nat. Rev. Mol. Cell Biol.* 12 (2011) 517–533.
- [11] S.L. Schmid, V.A. Frolov, Dynamin: functional design of a membrane fission catalyst, *Annu. Rev. Cell. Dev. Biol.* 27 (2011) 79–105.
- [12] S. Morlot, V. Galli, M. Klein, N. Chiaruttini, J. Manzi, F. Humbert, L. Dinis, M. Lenz, G. Cappello, A. Roux, Membrane shape at the edge of the dynamin helix sets location and duration of the fission reaction, *Cell* 151 (2012) 619–629.
- [13] A. Quan, A.B. McGeachie, D.J. Keating, E.M. van Dam, J. Rusak, N. Chau, C.S. Malladi, C. Chen, A. McCluskey, M.A. Cousin, P.J. Robinson, Myristyl trimethyl ammonium bromide and octadecyl trimethyl ammonium bromide are surface-active small molecule dynamin inhibitors that block endocytosis mediated by dynamin I or dynamin II, *Mol. Pharmacol.* 72 (2007) 1425–1439.
- [14] T. Hill, L.R. Odell, J.K. Edwards, M.E. Graham, A.B. McGeachie, J. Rusak, A. Quan, R. Abagyan, J.L. Scott, P.J. Robinson, A. McCluskey, Small molecule inhibitors of dynamin I GTPase activity: development of dimeric tyrosinostats, *J. Med. Chem.* 48 (2005) 7781–7788.
- [15] L.R. Odell, N. Chau, A. Mariana, M.E. Graham, P.J. Robinson, A. McCluskey, Azido and diazarynyl analogues of bis-tyrphostin as asymmetrical inhibitors of dynamin GTPase, *ChemMedChem* 4 (2009) 1182–1188.
- [16] J. Zhang, G.A. Lawrance, N. Chau, P.J. Robinson, A. McCluskey, From Spanish fly to room-temperature ionic liquids (RTILs): synthesis, thermal stability and inhibition of dynamin 1 GTPase by a novel class of RTILs, *New J. Chem.* 32 (2008) 28–36.
- [17] T.A. Hill, A. Mariana, C.P. Gordon, L.R. Odell, M.J. Robertson, A.B. McGeachie, N. Chau, J.A. Daniel, N.N. Gorgani, P.J. Robinson, A. McCluskey, Iminochromene inhibitors of dynamin I and II GTPase activity and endocytosis, *J. Med. Chem.* 53 (2010) 4094–4102.
- [18] L.R. Odell, D. Howan, C.P. Gordon, M.J. Robertson, N. Chau, A. Mariana, A.E. Whiting, R. Abagyan, J.A. Daniel, N.N. Gorgani, P.J. Robinson, A. McCluskey, The phthaladins: GTP competitive inhibitors of dynamin I and II GTPase derived from virtual screening, *J. Med. Chem.* 53 (2010) 5267–5280.
- [19] C.B. Harper, S. Martin, T.H. Nguyen, S.J. Daniels, N.A. Lavidis, M.R. Popoff, G. Hadzic, A. Mariana, N. Chau, A. McCluskey, P.J. Robinson, F.A. Meunier, Dynamin inhibition blocks botulinum neurotoxin type A endocytosis in neurons and delays botulism, *J. Biol. Chem.* 286 (2011) 35966–35976.
- [20] A. McCluskey, J.A. Daniel, G. Hadzic, N. Chau, E.L. Clayton, A. Mariana, A. Whiting, J. Lloyd, A. Quan, L. Moshkanbaryans, S. Perera, M. Chircop, A.B. McGeachie, M.T. Howes, R. Parton, M. Campbell, J.A. Sakoff, X. Wang, J.-Y. Sun, M.J. Robertson, F.M. Deane, T.H. Nguyen, F.A. Meunier, M.A. Cousin, P.J. Robinson, Building a better dynasore: the dyngos potently inhibit dynamin and endocytosis, *Traffic* 14 (2013) 1272–1289.
- [21] M.J. Robertson, G. Hadzic, J. Ambrus, D.Y. Pome, E. Hyde, A. Whiting, A. Mariana, L. von Kleist, N. Chau, V. Haucke, P.J. Robinson, A. McCluskey, The rhodadyns™ – novel inhibitors of dynamin GTPase, *ACS Med. Chem. Lett.* 3 (2012) 352–356.
- [22] T.A. Hill, C.P. Gordon, A.B. McGeachie, B. Venn-Brown, L.R. Odell, N. Chau, A. Quan, A. Mariana, J.A. Sakoff, M. Chircop, P.J. Robinson, A. McCluskey, Inhibition of dynamin mediated endocytosis by the dyngos—synthesis and

- functional activity of a family of indoles, *J. Med. Chem.* 52 (2009) 3762–3773.
- [23] C.P. Gordon, B. Venn-Brown, M.J. Robertson, K.A. Young, N. Chau, A. Mariana, A. Whiting, M. Chircop, P.J. Robinson, A. McCluskey, Development of second-generation indole-based dynamin GTPase inhibitors, *J. Med. Chem.* 56 (2012) 46–59.
- [24] M.J. Robertson, F.M. Deane, P.J. Robinson, A. McCluskey, Synthesis of a dynamin GTPases modulators toolkit: dynole 34-2, dynole-2-24 and dyngo 4a, *Nat. Prot.* 9 (2014) 851–870.
- [25] C.B. Harper, M.R. Popoff, A. McCluskey, P.J. Robinson, F.A. Meunier, Targeting membrane trafficking in infection prophylaxis: dynamin inhibitors, *Trends Cell Biol.* 23 (2013) 90–101.
- [26] D.A. Lanfranchi, E. Cesar-Rodo, B. Bertrand, H.H. Huang, L. Day, L. Johann, M. Elhabiri, K. Becker, D.L. Williams, E. Davioud-Charvet, *Org. Biomol. Chem.* 10 (2012) 6375–6387.
- [27] D. Belorgey, D.A. Lanfranchi, E. Davioud-Charvet, *Curr. Pharm. Des.* 19 (2013) 2512–2528.
- [28] J.B. Bael, G.A. Holloway, *J. Med. Chem.* 53 (2010) 2719–2740.
- [29] www.cancer.gov/drugdictionary (accessed 03.06.14.).
- [30] L. Margarucci, M.C. Monti, B. Fontanella, R. Riccio, A. Casapullo, Chemical proteomics reveals bolinaquinone as a clathrin-mediated endocytosis inhibitor, *Mol. Biosys.* 7 (2011) 480–485.
- [31] H. Yamada, T. Abe, S.-A. Li, S. Tago, P. Huang, M. Watanabe, S. Ikeda, N. Ogo, A. Asai, K. Takei, *N'*-[4-(dipropylamino)benzylidene]-2-hydroxybenzohydrazide is a dynamin GTPase inhibitor that suppresses cancer cell migration and invasion by inhibiting actin polymerization, *Biochem. Biophys. Res. Commun.* 443 (2014) 511–517.
- [32] S. Lee, K.Y. Jung, J. Park, J.H. Cho, Y.C. Kim, S. Chang, Synthesis of potent chemical inhibitors of dynamin, *Bioorg. Med. Chem. Lett.* 20 (2010) 4858–4864.
- [33] M. Otomo, K. Takahashi, H. Miyoshi, K. Osada, H. Nakashima, N. Yamaguchi, Some selective serotonin reuptake inhibitors inhibit dynamin I guanosine triphosphatase (GTPase), *Biol. Pharm. Bull.* 31 (2008) 1489–1495.
- [34] G.M. Morris, R. Huey, W. Lindstrom, M.F. Sanner, R.K. Belew, D.S. Goodsell, A.J. Olson, AutoDock4 and AutoDockTools4: automated docking with selective receptor flexibility, *J. Comput. Chem.* 30 (2009) 2785–2791.
- [35] S. Bayen, N. Barooah, R.J. Sarma, T.K. Sen, A. Karmakar, J.B. Baruah, Synthesis, structure and electrochemical properties of 2,5-bis-(alkyl/arylamino)1,4-benzoquinones and 2-arylamino-1,4-naphthoquinones, *Dyes Pigments* 75 (2007) 770–775.
- [36] L.C.A. Barbosa, U.A. Pereira, C.R.A. Maltha, R.R. Teixeira, V.M.M. Valente, J.R.O. Ferreira, L.V. Costa-Lotufo, M.O. Moraes, C. Pessoa, Synthesis and biological evaluation of 2,5-bis-(alkylamino)-1,4-benzoquinones, *Molecules* 15 (2010) 5629–5643.
- [37] X. Liu, M. Tu, R.S. Kelly, C. Chen, B.J. Smith, Development of a computational approach to predict blood-brain barrier permeability, *Drug Metab. Dispos.* 32 (2004) 132–139.
- [38] C. Acharya, P.R. Seo, J.E. Polli, A.D. MacKerell, Computational model for predicting chemical substituent effects on passive drug permeability across parallel artificial membranes, *Mol. Pharm.* 5 (2008) 818–828.
- [39] A. Alex, D.S. Millan, M. Perez, F. Wakenhut, G.A. Whitlock, Intramolecular hydrogen bonding to improve membrane permeability and absorption in beyond rule of five chemical space, *MedChemComm* 2 (2011) 669–674.
- [40] B. Kuhn, P. Mohr, M. Stahl, Intramolecular hydrogen bonding in medicinal chemistry, *J. Med. Chem.* 53 (2010) 2601–2611.
- [41] M.F. Sanner, Python: a programming language for software integration and development, *J. Mol. Graph. Model.* 17 (1999) 57–61.
- [42] A.-M. Osman, Benzodioxazoles, *J. Am. Chem. Soc.* 79 (1957) 966–968.
- [43] L.F. Fieser, E. Berliner, F.J. Bondhus, F.C. Chang, W.G. Dauben, M.G. Ettlinger, G. Fawaz, M. Fields, C. Heidelberger, H. Heymann, W.R. Vaughan, A.G. Wilson, E. Wilson, M.-i. Wu, M.T. Leffler, K.E. Hamlin, E.J. Matson, E.E. Moore, M.B. Moore, H.E. Zaugg, Naphthoquinone antimalarials. IV–XI. Synthesis, *J. Am. Chem. Soc.* 70 (1948) 3174–3215.
- [44] C.D.S. Lisboa, V.G. Santos, B.G. Vaz, N.C. de Lucas, M.N. Eberlin, S.J. Garden, C–H functionalization of 1,4-naphthoquinone by oxidative coupling with anilines in the presence of a catalytic quantity of copper(II) acetate, *J. Org. Chem.* 76 (2011) 5264–5273.
- [45] E. Grossmann, Über die einwirkung der drei isomeren aminophenole auf α -naphthochinon, *J. Prakt. Chem.* 92 (1915) 370–390.
- [46] C.R. Tindale, Reactions of biogenic amines with quinones, *Aust. J. Chem.* 37 (1984) 611–617.
- [47] K.W. Wellington, P. Steenkamp, D. Brady, Diamination by N-coupling using a commercial *Laccase*, *Bioorg. Med. Chem.* 18 (2010) 1406–1414.
- [48] M.G. Johnson, H. Kiyokawa, S. Tani, J. Koyama, S.L. Morris-Natschke, A. Mauger, M.M. Bowers-Daines, B.C. Lange, K.-H. Lee, Antitumor agents-CLXVII. Synthesis and structure-activity correlations of the cytotoxic anthraquinone 1,4-bis-(2,3-epoxypropylamino)-9,10-anthracenedione, and of related compounds, *Bioorg. Med. Chem.* 5 (1997) 1469–1479.
- [49] A.E. Mathew, R.K.Y. Zee-Cheng, C.C. Cheng, Amino-substituted *p*-benzoquinones, *J. Med. Chem.* 29 (1986) 1792–1795.
- [50] R.M. Acheson, B.F. Sansom, The reaction between quinones and anthranilic acids, *J. Chem. Soc.* (1955) 4440–4443.
- [51] J.D. Adkins, T.A. Eaton, A.J. Perez, Potential aminoquinone inhibitors of CE and BMI/carbon fiber/aluminum composite galvanic degradation, in: 33rd International SAMPE Technical Conference, vol. 33, 2001, pp. 911–923.
- [52] H. Suida, Über anilindochinone, *Justus Liebigs Ann. Chem.* 416 (1918) 113–163.